5101-284
Flat-Plate Solar
Array Project

DOE/JPL-1012-120
Distribution Category UC-63b

Chemical Bonding Technology: Direct Investigation of Interfacial Bonds

J.L. Koenig
F.J. Boerio
E.P. Plueddemann
J. Miller
P.B. Willis
E.F. Cuddihy

January 1986

Prepared for
U.S. Department of Energy
Through an Agreement with
National Aeronautics and Space Administration
by
Jet Propulsion Laboratory
California Institute of Technology
Pasadena, California

JPL Publication 86-6

5101-284
Flat-Plate Solar
Array Project

DOE/JPL-1012-120
Distribution Category UC-63b

Chemical Bonding Technology: Direct Investigation of Interfacial Bonds

J.L. Koenig
F.J. Boerio
E.P. Plueddemann
J. Miller
P.B. Willis
E.F. Cuddihy

January 1986

Prepared for
U.S. Department of Energy
Through an Agreement with
National Aeronautics and Space Administration
by
Jet Propulsion Laboratory
California Institute of Technology
Pasadena, California

JPL Publication 86-6

Prepared by the Jet Propulsion Laboratory, California Institute of Technology, for the U.S. Department of Energy through an agreement with the National Aeronautics and Space Administration.

The JPL Flat-Plate Solar Array Project is sponsored by the U.S. Department of Energy and is part of the National Photovoltaics Program to initiate a major effort toward the development of cost-competitive solar arrays.

This document reports on work done under NASA Task RE-152, Amendment 419, DOE/NASA IAA No. DE-AI01-85CE89008.

ABSTRACT

This is the third Flat-Plate Solar Array (FSA) Project document reporting on chemical bonding technology for terrestrial photovoltaic (PV) modules. The impetus for this work originated in the late 1970s when PV modules employing silicone encapsulation materials were undergoing delamination during outdoor exposure. At that time, manufacturers were not employing adhesion promoters and, hence, module interfaces in common with the silicone materials were only in physical contact and therefore easily prone to separation if, for example, water were to penetrate to the interfaces. Delamination with silicone materials virtually vanished when adhesion promoters, recommended by silicone manufacturers, were used.

With the decrease in use of silicone encapsulants, and the increase in use of hydrocarbon encapsulants such as ethylene vinyl acetate (EVA), the need developed for adhesion promoters specifically developed for these new materials. The adhesion promoters being developed for EVA-type materials are based on organosilanes, which generate primary chemical bonds at the interface, that is, chemical bonding. These adhesion promoters are commonly referred to as "primers."

The first report on this subject (Chemical Bonding Technology for Terrestrial Solar Cell Modules, by E.P. Plueddeman, JPL 5101-132, dated September 1, 1979) described the chemistry of primers based on organosilane chemistry, and the second report (Chemical Bonding Technology for Terrestrial Photovoltaic Modules, by D.R. Coulter, E.F. Cuddihy, and E.P. Plueddeman, JPL Publication 83-86, dated November 15, 1983) described chemical bonding theories, and also included a listing of candidate primer and adhesive systems being investigated for all of the various module interfaces. This report describes the activities related to the direct investigation of chemically bonded interfaces.

ACKNOWLEDGMENT

The authors thank the following companies for courteously supplying solar cells used for the adhesion studies discussed in this Project report: SOLEC International, Hawthorne, California; Spectrolab, Inc., Sylmar, California; and Tideland Signal, Houston, Texas.

ABBREVIATIONS AND ACRONYMS

AES	Auger electron spectroscopy
DRIFT	diffuse reflectance infrared spectroscopy
EDAX	energy dispersive x-ray analysis
EVA	ethylene vinyl acetate
FSA	Flat-Plate Solar Array
FTIR	Fourier transform infrared spectroscopy
IPN	Interpenetrating Polymer Network
OH	organic alcohols
OR	organic ethers
PV	photovoltaic
RAIR	reflection absorption infrared spectroscopy
XPS	x-ray photoelectron spectra

CONTENTS

Figures

Figures (Cont'd)

Figures (Cont'd)

Tables

SECTION I

INTRODUCTION

Adhesives and primers are necessary for the high reliability bonding of photovoltaic (PV) module interfaces to ensure structural integrity and long life. The adhesion between the pottant and other components (i.e., substrate, superstrate, and outer cover) must have adequate bond strength to hold the module components together, with a Flat-Plate Solar Array (FSA) Project goal of 30 years of outdoor service life. Accordingly, the material components of the module should be held together by strong chemical bonding, with the interfacial bonding being resistant to delamination from the combined weathering actions of moisture, temperature, and ultraviolet light.

Toward this end, Dow Corning (Dr. Edwin Plueddemann) is developing chemical bonding agents based on organosilane chemistry called silane coupling agents, which are chemically bifunctional. Using glass and ethylene vinyl acetate (EVA) as an example, one of the chemical groups on a silane coupling agent is designed to react with glass, while the other chemical group will react with EVA. Thus, the interfacial bonding is accomplished by actual primary chemical bonds bridging across the interface.

In general, the silanes employed for these coupling agents are typically resistant to deterioration by ultraviolet light, and therefore the main concern is from hydrothermal deterioration over a long exposure time outdoors. Ordinarily the quality (strength) of bonded materials is monitored by mechanical peel tests, where failure is defined as cohesive if it occurs in either of the two bonded materials, or adhesive if failure occurs in the interfacial region. Using silane coupling agents and, again, EVA and glass as an example, failures of control and hydrothermally aged EVA/glass specimens are normally cohesive within the EVA (References 1 and 2). That is, the bond strength exceeds the tensile strength of EVA. Thus, accelerated hydrothermal aging may be decreasing the bond strength, but if it continues to exceed the EVA's tensile strength, it cannot be monitored by mechanical testing.

Dr. Koenig at Case Western Reserve University has been pioneering techniques based on Fourier Transform Infrared (FTIR) spectroscopy to investigate chemically bonded interfaces for information related to bond population. The first part of this Project document is a report on Dr. Koenig's FTIR activities at Case Western, in collaboration with Dr. Miller. During this work, it was found necessary to disperse small diameter glass beads in EVA in order to increase the surface-to-volume ratio of test specimens for FTIR detection. Of technical significance, it was recently found (Reference 2) that the equilibrium water absorption of these composite specimens was a strong function of the level of chemical bonding. For example, one series of unprimed EVA/glass specimens reported in Reference 2 absorbed nearly 2000 wt % water at 60°C, whereas a primed EVA/glass specimen absorbed only 35 wt % water at 60°C. For future work, this finding offers a possibility for monitoring changes in the chemically bonded interface from simple measurements of equilibrium-absorbed water contents of aged specimens.

Dow Corning has successfully developed a silane coupling agent formulation (called a "primer") for EVA and glass. This primer is designated A-11861, and experimental quantities are available from Springborn Laboratories. Separately, work continues at Dow Corning to develop primers for bonding EVA to solar cells, and solar cell metallization materials, such as aluminum. The reason for this activity is that silane coupling agents also appear to passivate metal surfaces against corrosion (References 3, 4, 5, and 6).

Dr. Boerio at the University of Cincinnati has been pioneering techniques based on ellipsometry and reflection absorption infrared (RAIR) spectroscopy to investigate chemically bonded interfaces between metals and polymers. The second part of this Project document is a report on activities at the University of Cincinnati. Of significance is the apparent finding that the silane coupling agent employed in the A-11861 EVA/glass primer may be effective for bonding EVA to the aluminized back surfaces of solar cells, and may also be effective in stopping environmentally induced corrosion of this aluminum. Thus, a self-priming EVA formulated with this silane coupling agent would work with both glass and solar cells. Dr. Boerio's work indicates that the silane coupling agent in A-11861 only works between EVA and the aluminum on solar cells, and not between EVA and any other aluminum. Although preliminary, new insights into the general area of bonding to aluminum may result from this work.

SECTION II

CHEMICAL BONDING BETWEEN GLASS AND ETHYLENE VINYL ACETATE (EVA)

In order to meet the required specifications, encapsulated PV modules must remain intact for 30 years, reliably resisting delamination and separation of any of the component materials. For such long outdoor life, strong weather-stable interfacial bonds must be formed between the component materials. In order to achieve such stability, adhesion promoters are used to enhance the strength and durability of such bonds. The chemical bonding technology has been described in two previous reports (References 7 and 8) and should be reviewed prior to this report in order to ascertain the current status with respect to materials, adhesion promoters, and process considerations.

Characterizing the chemical nature of the adhesion between different materials is challenging and difficult. The first problem is the small concentration of interfacial bonds relative to the bulk. The second problem is that the interfacial bonds are generally quite similar to those of the bulk, making the detection more difficult. Efforts have been made to understand the mechanism of the coupling agent action. The earliest efforts focused primarily on the role of the coupling agent in improving the mechanical properties. Many potential coupling agents were tested and the results generated a number of explanations ranging from improvements in surface wettability, presence of acid-base reactions, and the formation of chemical bonds. Each of these postulates describe some aspect of the response of the mechanical properties to the different silanes and their processes, but none of them are sufficient to explain all of the observations.

Over the past 40 years, many techniques have been used to evaluate the interfacial chemistry of materials. Some of these techniques include microscopy, contact angle measurements, gel permeation chromatography, zeta potentials, heats of immersion, and radioactive labeling. Although these techniques are precise in their analysis, the major limitation is that either they do not yield molecular structural information or have sufficient sensitivity to detect monolayers. Infrared spectroscopy has been widely used as a technique to study surfaces (References 9 and 10) and with the advent of FTIR, it has become an even more effective tool because of the high sensitivity, excellent structural resolution, simple sampling techniques, and computer processing of the spectra. The effectiveness of FTIR for the study of the interfaces of glass fiber composites has been demonstrated (References 11, 12, 13, and 14). On this basis, it was selected for use to study the interfacial bonding of glass/EVA in terrestrial PV modules.

There are a number of factors that determine the chemical basis of the adhesion. The nature of the surface functionality of the bonding materials determines the potential for chemical modification of the adhesion. A necessary prerequisite for molecular design of the adhesive interfacial bonds is knowledge of the surface functionalities. Using FTIR spectral reflection techniques, insights into the chemical nature of the surface can be obtained.

Adhesion is most often promoted using a coupling agent that is specific for the materials to be bonded. A coupling agent, as the name implies, is a molecule that couples together two different molecules. This molecular fastening is made for the purposes of promoting adhesion between the two molecules which are generally found at an interface between two surfaces. A coupling agent is bifunctional so that each end of the molecule can connect with the molecules of the surfaces that are being bonded. A especially useful class of coupling agents is the organosilanes, where one end of the molecule has organic functionality to react with organic surfaces, and the other end is inorganic to react with inorganic surfaces.

Silane coupling agents have the general form $X-(CH_2)_3-Si-(OR)_3$. The functional group X can be varied to optimize the reactivity with the polymer matrix to be connected to the glass (Figure 1). The organic ethers (OR) groups are short chain ethers that are readily hydrolyzed in water that is slightly acidic to alcohols leaving a silanetriol group which is very reactive with itself (condensation/polymerization) and the glass surface. In industrial practice, the silanes are dissolved in water or alcohol and the glass is treated with a dilute (1% by weight) solution. This dilute solution is commonly referred to as a "primer." The amount of silane on the surface of the glass is very small and its molecular structure is a function of the treating and drying conditions of the industrial process.

Beginning in the early 1960s, questions were being asked concerning the nature of the coupling agent on the surfaces. Is the coupling agent bound to the substrate material? If so, is the type of bonding important to the adhesion? How much coupling agent is needed to yield maximum adhesion? Does the coupling agent chemically react with the polymer matrix? Is the amount of chemical reaction important to the adhesion? Could the performance of the coupling agent be controlled by the treating conditions? These questions can be answered using FTIR in the appropriate manner.

The questions of lifetime of the adhesive bond are also complex. Is the coupling agent present on the substrate material after exposure to water/humidity? Is the structure of the coupling agent modified by the presence of water? Does the water preferentially attack the interfacial bonds? Questions of this kind can be answered with accelerated exposure tests combined with FTIR spectroscopic characterization.

The model of the adhesive joint for EVA/glass can be considered as a sandwich structure (Figure 2) with a series of layers. These layers include:

(1) The bulk glass substrate.

(2) An interface between the glass and the coupling agent.

(3) A region of bulk polysiloxane (interphase).

(4) An interface between the coupling agent and the EVA.

(5) The bulk EVA region.

It is convenient to discuss the results of this report in terms of these components as each plays a role in the ultimate properties of the adhesion.

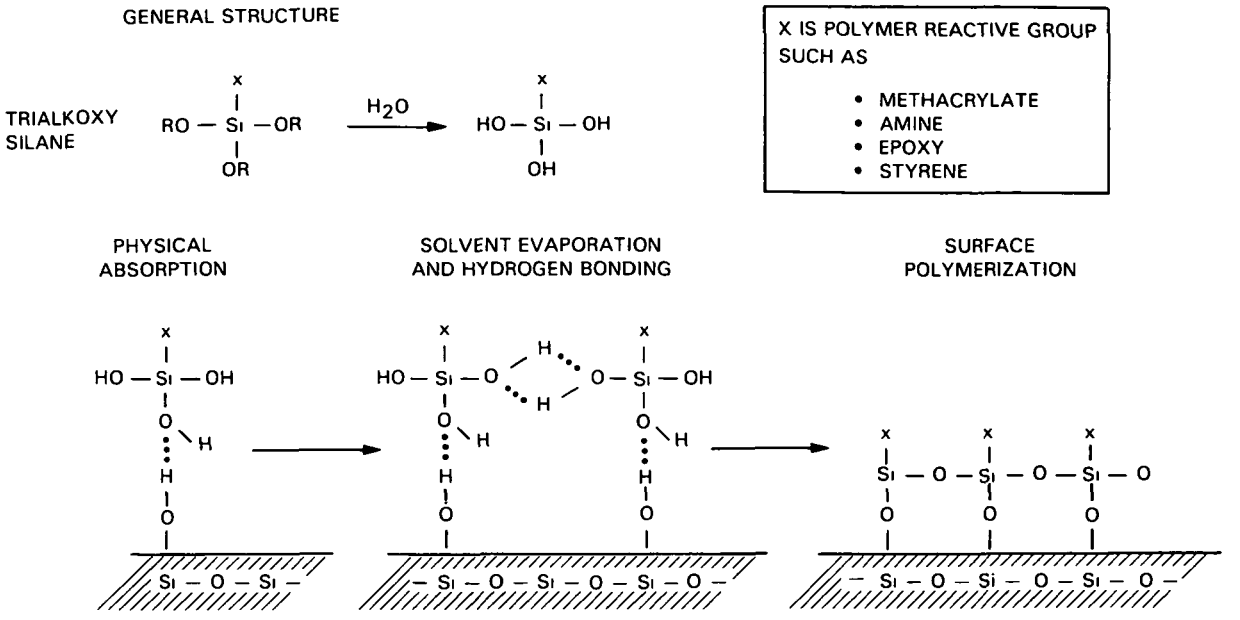

Figure 1. Bonding of Silane Coupling Agents to Glass

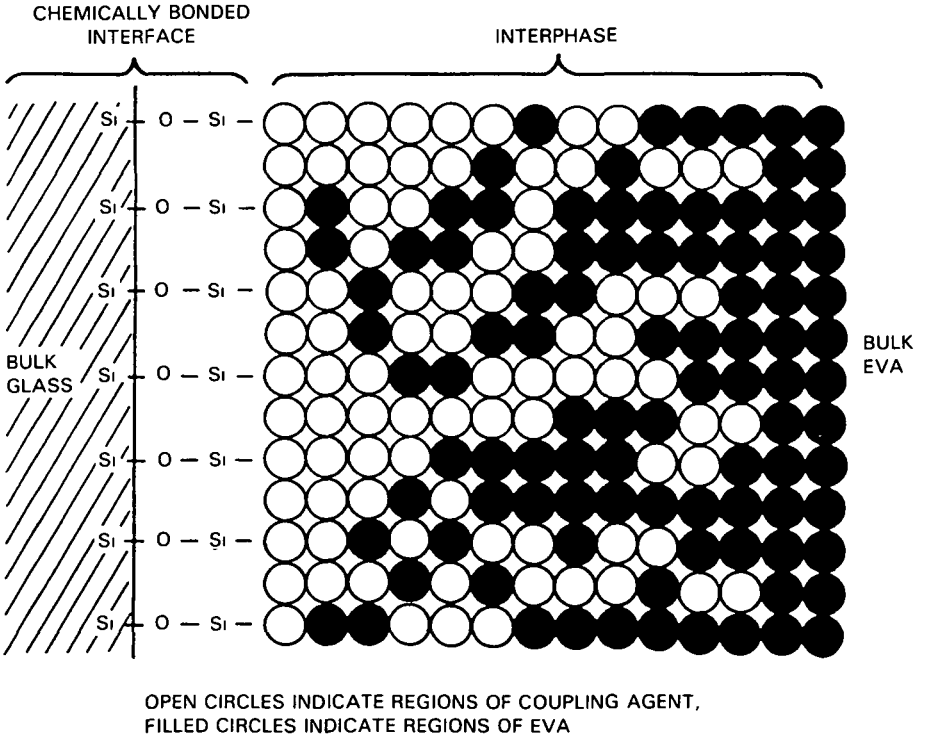

Figure 2. Interdiffusion Model for a Silane-Primed EVA/Glass Joint

A. FOURIER TRANSFORM INFRARED (FTIR) SPECTROSCOPY OF SURFACES AND INTERFACES

FTIR provides great potential for surface studies. Infrared spectroscopy is one of the most versatile, widely used techniques for the determination of molecular structure. Recent advances in infrared spectroscopy also offer new sampling methods to characterize surfaces of materials and absorbed species on the surfaces. These methods include reflection and emission techniques. These new sampling techniques are further enhanced using FTIR, rather than the conventional dispersive-type spectrometer. Moreover, data processing techniques such as spectral subtraction and computer-scale expansion allow improved selectivity.

In FTIR, a Michelson interferometer is used instead of the prisms and slits used in conventional infrared spectroscopy. Obviously, a slitless spectrometer has an advantage in energy throughput. However, a more pronounced advantage comes from the so-called Fellget's advantage, or multiplex advantage, which allows all resolution elements to be detected simultaneously throughout the spectral range; a dispersive instrument receives a signal only from one resolution element at a time. The signal-to-noise ratio is proportional to the square root of the number of resolution elements (i.e., the spectral range divided by the resolution). Each scan takes only 1 s, so the signal-to-noise ratio can be further increased by consecutive accumulation of scans as the scan rate is on the order of 1 s.

In FTIR, an interferogram is obtained that consists of many waves of different frequencies. This interferogram is collected as a function of retardation time of the moving mirror that separates the light frequencies according to their time of travel which is a function of the wavelength. This interferogram is the Fourier transform of the desired infrared spectrum. The spectrum is digitized so that it can be stored on the dedicated minicomputer for further data processing.

1. Advantages of FTIR for Surface Studies

Surface studies are always a challenge to the limitations of instruments and methods. Surface studies require sufficient sensitivity, a high signal-to-noise ratio, and selectivity. It is apparent that the amount of material at the surface (four or five atomic layers) is negligible compared to the bulk. In a transmission experiment with a pressed disc, the bulk equivalent of 103 monolayers must be penetrated. Therefore, the suppression of the signal of the bulk (i.e., selectivity) is an essential factor. Furthermore, the dynamic range of the instruments and techniques need to be large, as is the case for FTIR.

2. Sampling Techniques for FTIR Spectroscopy Studies

The various techniques for the study of surfaces using FTIR have been reviewed recently (Reference 15). For this work, two techniques were used: transmission and diffuse reflectance (DRIFT). A discussion of the transmission technique is unnecessary, as the technique is routine. However, the digital subtraction approach is important and will be described in the next section.

Although diffuse reflection sampling has been used in the ultraviolet and visible region for a long time, it was only with the increased sensitivity of FTIR that diffuse reflectance was possible in the infrared region. The basic principle behind diffuse reflectance spectroscopy is that light incident upon a solid or powdered surface is diffusely scattered in all directions (Reference 16). The scattered light is collected with the proper optical setup and directed to the infrared detector for analysis. Thus, diffuse reflectance permits the study of surfaces of particulate and rough samples to be studied. The principal advantages of diffuse in the infrared are: (1) it is a surface spectroscopy technique which is quantitative, and (2) it allows opaque and/or strongly absorbing solids and other problem samples to be studied with relative ease.

Diffuse reflectance rather than transmission methods were used in this study for several reasons, the first and foremost being the increased sensitivity of diffuse reflectance to the coupling agent on the glass surface. This sensitivity made the observation of very small amounts of coupling agents possible. These measurements would have been difficult with ordinary transmission techniques. Also, it is not necessary to alter the sample in any way to obtain the spectrum. For transmission studies, the sample must be ground to a small particle size, dispersed in potassium bromide, and pressed into a pellet. The grinding process may destroy those chemical bonds of direct interest in adhesion. Normally, in diffuse reflectance, the powdered sample is mixed with powdered KBr and placed in a sample chamber.

3. Data Processing Techniques

In spite of the development of the reflection methods indicated above, the study of surfaces using transmission measurements remains the most widely used technique, particularly for inorganic and organic substrates which can be prepared in the appropriate form. It was recognized that absorbance subtraction could be used for the study of surfaces. If the infrared spectrum of a bulk sample is obtained and the same bulk sample is given a surface treatment, spectral subtraction can be used to remove the interference. The bulk phase and the resultant difference spectrum would then reflect the differences in the surfaces before and after treatment. If the untreated sample is subtracted from the treated sample, positive absorbance bands would rise from the higher concentration of surface species in the treated sample, and negative bands from species would be preferentially found in the untreated surfaces. After the isolation of the difference spectrum, the absorbance scale can be expanded to one-third of the signal-to-noise ratio, as the strong absorbing bands due to the bulk have been removed, giving a very high sensitivity for the technique. In this manner, one can determine the nature of the chemical reactions occurring with surface treatments.

B. EXPERIMENTAL PROCEDURES (MATERIALS)

Sunadex glass is preferred for the solar modules, but it was anticipated and confirmed that the flat glass would not have sufficient surface area to allow detection of the coupling agent by FTIR, so particulate glass was used to increase the surface-to-volume ratio. The specimens were prepared by dispersing high loadings of extremely fine, essentially spherical glass

powder[1] in the EVA and curing as usual to "set" the bond chemistry. The test specimens were prepared to determine the effects of hydrothermal aging (heat and water) on glass/primer/EVA bonds. These specimens were designed for use in a parallel program in which the decay of mechanical properties (bond strength) could be measured with simultaneous spectroscopic investigation of the interface to follow the chemistry.

The test specimens consisted of both primed and unprimed glass powders and both EVA (Elvax 150) and polyethylene were used as the polymers. The glass powders were first washed in dilute mineral acid to remove alkaline residues on the surface, then dried and treated with primer[2] until a total of 2 wt % of active primer was deposited on the surface. The treated glass was then used to prepare the formulations described in Table 1.

Tensile bars were cut from cured molded plaques and then exposed to hydrothermal aging conditions by immersion in water at the times and temperatures described in Table 2. The test bars resulting from these exposures were then tested for mechanical properties before and after drying, and also for spectroscopic examination.

C. FTIR SPECTROSCOPY STUDIES OF UNAGED EVA/GLASS INTERFACES

The FTIR spectra of each of the components in the EVA/glass-coupling agent has been isolated as indicated in Figure 3. Spectrum A is EVA. The spectrum shown as B is obtained from the total system containing all of the components. Spectra C are the spectra of the interfaces involving the silane at the EVA/glass interface. Spectrum D is the γ-MPS coupling-agent interphase, and Spectrum E is the particulate glass. The discussion that follows will explain the nature of these spectra and the information they contain.

1. Glass

The diffuse reflectance spectrum (DRIFT) of the untreated or pristine glass is shown in Figure 4. The strong bands observed below 1320 cm^{-1} are the symmetric and asymmetric Si-O-Si stretching modes. The spectrum shows little absorption in the organic alcohols (OH) stretching region indicating very few siloxyl groups on the surface.

---

[1]Potter's Industries, Hasbrouck Heights, New Jersey, Product 5000. Spherical A-glass powder, 400 mesh, mean particle diameter approximately 20μ, mean surface area, 0.269 m^2/g.

[2]Springborn Laboratories, Primer A11861, consisting of 90% Dow Corning Z-6030, 9% of Benzyl dimethylamine catalyst, and 1% Lupersol TBEC peroxide. These active ingredients are dissolved in methyl alcohol to give a 1% solution. Equivalent to approximately 100 monolayers of silane. The Z-6030 coupling agent is chemically γ-methacryloxypropyltrimethoxy silane, commonly referred to as γ-MPS.

Table 1. Adhesive Bonding Test Formulations

	18181-A	18181-B	18181-C	18181-D
Elvax 150 (EVA)	100	100	--	--
Chemplex 6230 polyethylene	--	--	100	100
Lupersol TBEC	1.5 PHR	1.5 PHR	1.5 PHR	1.5 PHR
Unprimed glass beads	110.8 PHR	--	110.8 PHR	--
Primed glass beads	--	110.8 PHR	--	110.8 PHR
Volume percent loading	30%	30%	30%	30%
Cure: 150°C/20 min	- - - - - - - - - - - -		all	- - - - - - - - -

PHR = Parts per hundred parts EVA or polyethylene.

Table 2. Hydrothermal Aging Conditions

Water Temperature	Hours					
	100	250	500	1000	2000	5000
40°C	X		X		X	X
60°C	X	X	X		X	
80°C	X	X	X	X		

X = Time and temperature conditions tested.

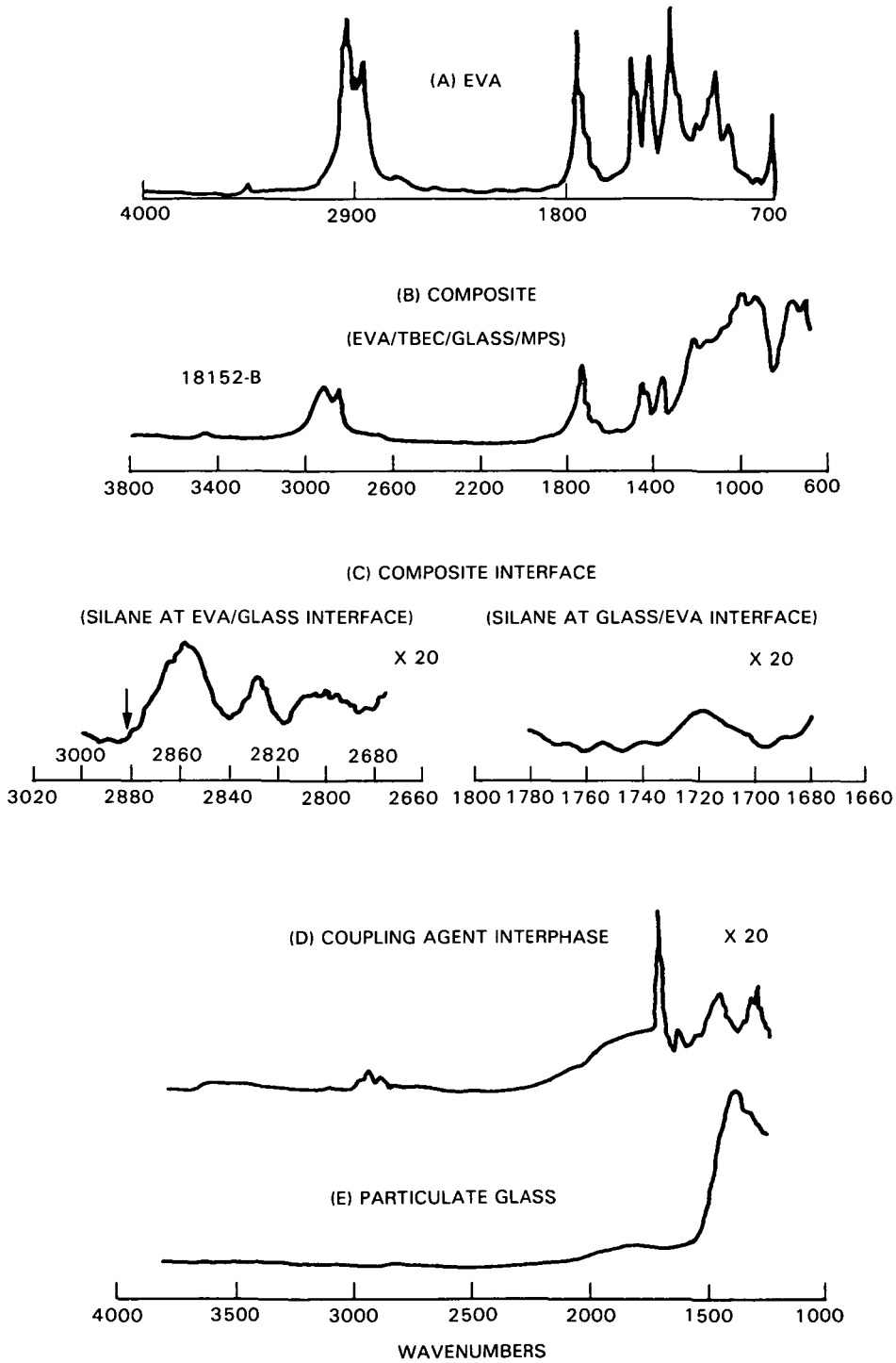

Figure 3. Diffuse Reflectance Spectrum of Material Components and Composites

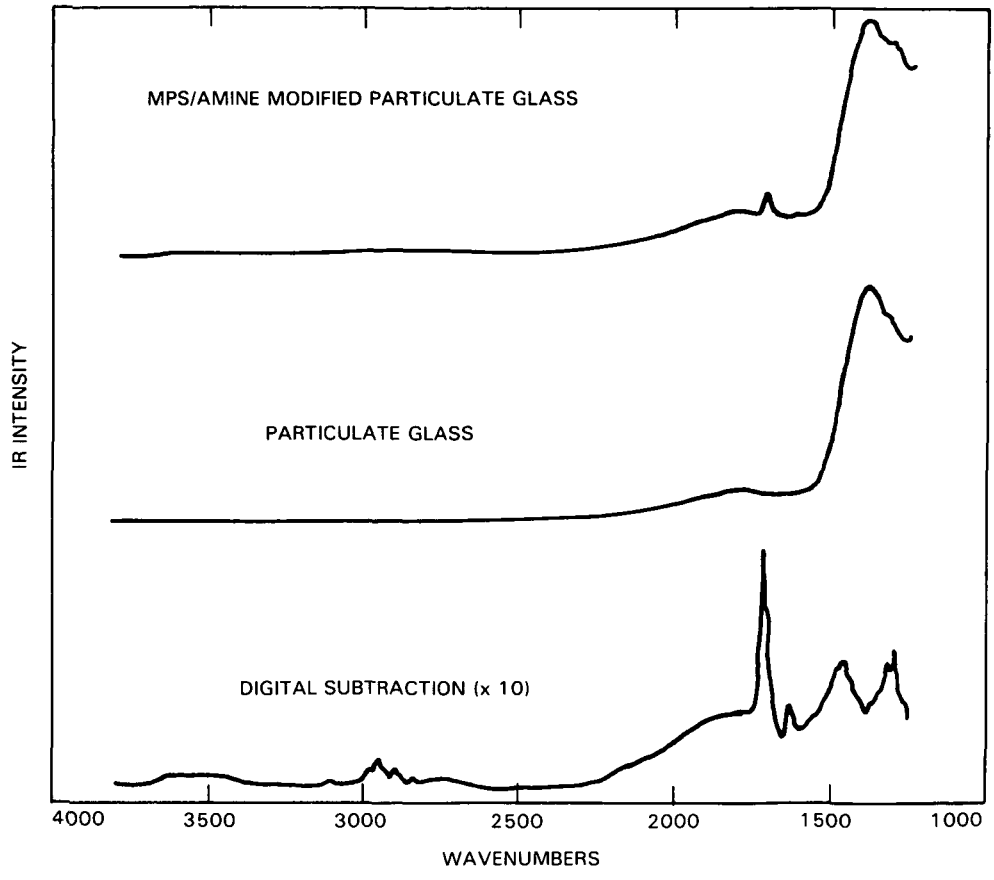

Figure 4. Diffuse Reflectance FTIR Spectra of Y-MPS/Amine Modified Particulate Glass, the Untreated Particulate Glass, and the Difference Spectrum Showing the Presence of the Y-MPS on the Surface of the Glass

2. Coupling Agent on Glass Surface

The spectrum of the treated glass is shown in Figure 3 (shown as C). The bottom spectrum (shown as E) shows the scale expanded (X10) difference obtained by subtracting the spectrum of the untreated glass from the treated glass. This difference reflects the spectrum of the coupling agent on the glass surface.

The amount of coupling agent on the surface is determined by the concentration of the coupling agent in the aqueous solution. The DRIFT spectra of particulate glass that has been treated with different concentrations of the Y-MPS/amine agent are shown in Figure 5. Below a weight percent of 0.03, no coupling agent is detected on the surface. The amount on the surface increases as the concentration of treating solution increases. Figure 6 shows the relationship between the integrated intensity of the carbonyl band of the Y-MPS and the weight percent loading in the treating solution. A nearly linear correlation is found. Calculations indicate that at 1% loading, there are approximately 50 monolayers of coupling agent on the surface. This result is in agreement with previous measurements of this kind for glass fibers (Reference 17).

Figure 7 shows the band assignments in this region with the 1720 cm^{-1} band being assigned to the free carbonyl stretching mode and the 1700 cm^{-1} to the H-bonded carbonyl mode. This latter mode is probably associated with

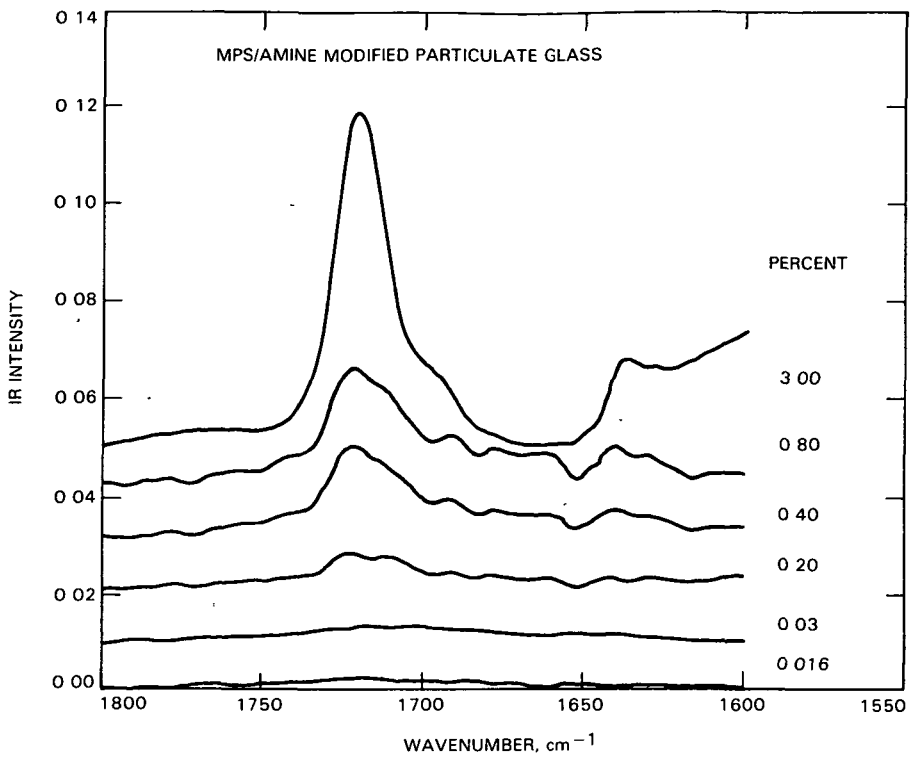

Figure 5. DRIFT Spectrum of Y-MPS/Amine Modified Particulate Glass Showing the Increase in the Intensities of the Y-MPS with the Percent Loading of the Treating Solution

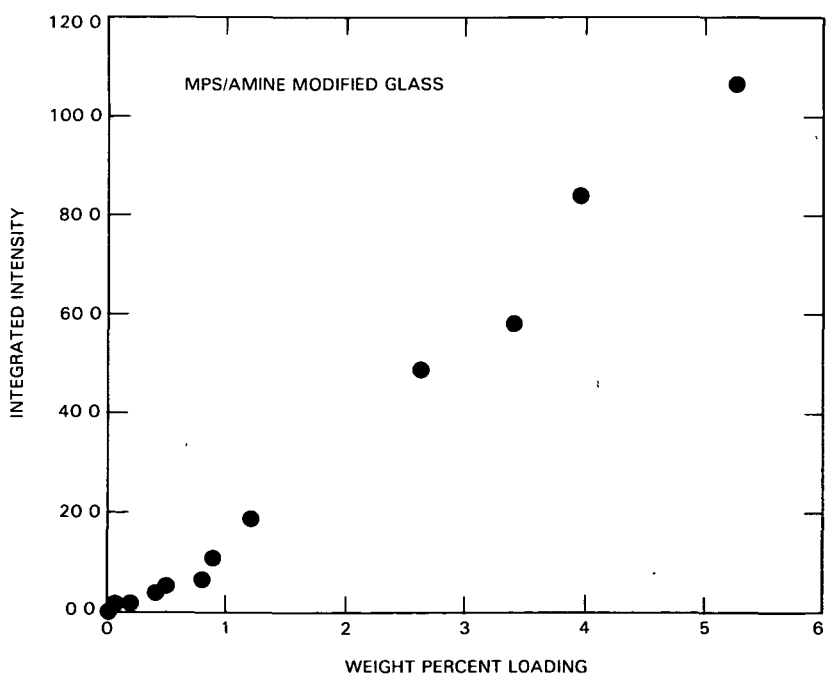

Figure 6. Plot of the Integrated Intensity of the Carbonyl Band of Y-MPS on the Surface of the Particulate Glass as a Function of Weight Percent Loading of the Particulate Glass

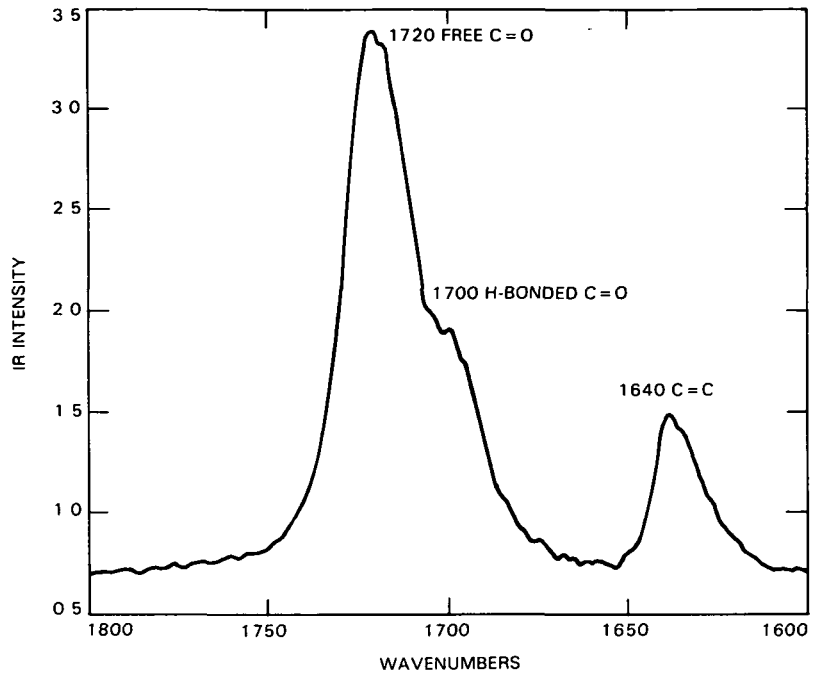

Figure 7. Spectrum of Y-MPS on the Surface of the Glass in the Carbonyl Stretching Region Showing the Vibrational Band Assignments Including the C = O and C = C Modes. (The band at 1700 cm^{-1} is the carbonyl stretching mode arising from hydrogen bonding of the initial layer of Y-MPS to the silanols on the glass surface.)

the hydrogen bonding of the Y-MPS to the glass surface and arises primarily from the first monolayer of Y-MPS on the surface of the glass. The weaker band at 1640 cm^{-1} is assigned to the C = O stretching mode of the Y-MPS. This band (at 1640 cm^{-1}) is especially useful for following the polymerization of the Y-MPS to polymethacrylate.

3. Hydrothermal Stability of the Glass/Coupling Agent Interface

In an effort to determine the hydrothermal stability of the coupling agent on the glass surface, the treated glass powder was exposed to water at 80°C for 3 h, and the spectra measured afterward. The amount of coupling agent remaining on the surface is indicative of the relative hydrolytic stability of the coupling agent on the surface (Reference 18). Figure 8 shows the results of these measurements by comparing the amount of coupling agent on the surface before and after water exposure. The results indicate that with the amine catalyst, very little of the coupling agent is removed by the water exposure, although without the amine (except for the initial monolayer on the surface), all of the coupling agent is removed. The behavior observed for the coupling agent on glass fibers without amine catalyst indicates that most of the coupling agent can be easily removed (Reference 19). The amine catalyst is apparently effective in condensing and crosslinking the coupling agent interphase on the surface making the interphase hydrothermally stable.

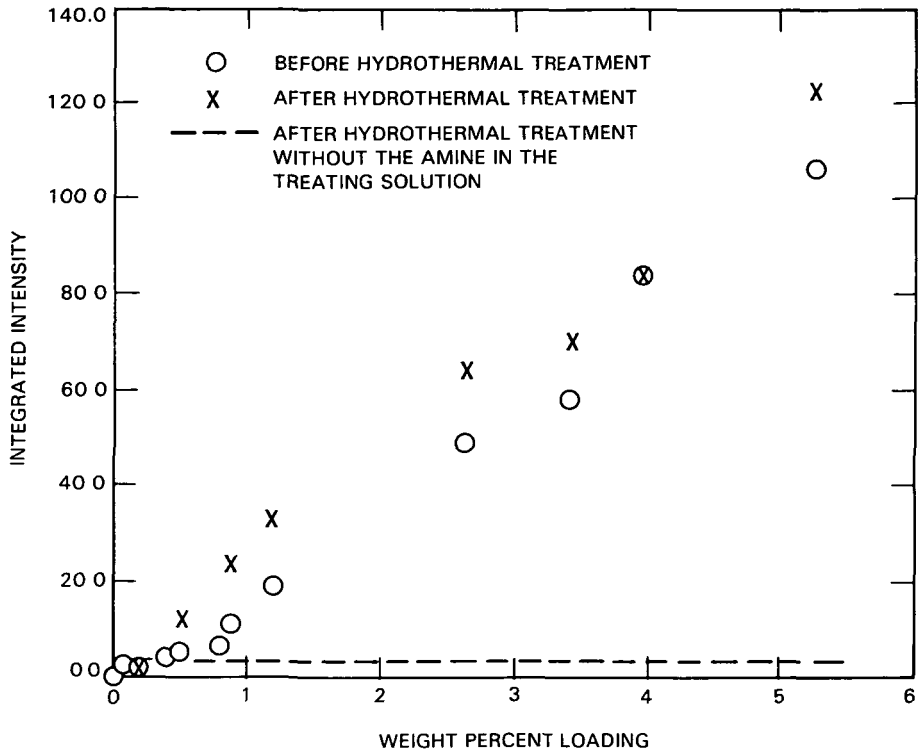

Figure 8. Plot of the Integrated Carbonyl Band as a Function of Weight Percent Loading

However, it has been observed that the nature of the glass surface plays an important role in the hydrothermal stability. Figure 9 shows the spectrum before and after hydrothermal treatment of Sunadex Glass, and it is apparent that nearly all of the coupling agent has been removed. This problem can be alleviated by an acid pretreatment of the glass as shown in Figure 10. In the latter case, the only effect of the water is to hydrolyze the residual methoxy groups of the coupling agent.

4. EVA

The spectrum of EVA obtained by DRIFT is shown in Figure 11. The bands near 2800 cm^{-1} are the carbon-hydrogen stretching modes of the polyethylene backbone. The sharp band near 1800 cm^{-1} is associated with the carbonyl group of the vinyl acetate copolymer, and the remaining bands are hydrocarbon in nature.

5. EVA/Glass Interface

In Figure 12, the spectrum of an EVA/glass composite is shown as well as the spectrum of the silane modified glass. The final spectrum is the subtracted spectrum which isolates the spectrum of the silane at the EVA/glass interface. It is apparent that the silane carbonyl mode can be observed, but the overlap of the acetate carbonyl band is extensive, making quantitative measurements difficult. In the carbon-hydrogen stretching region, it can be

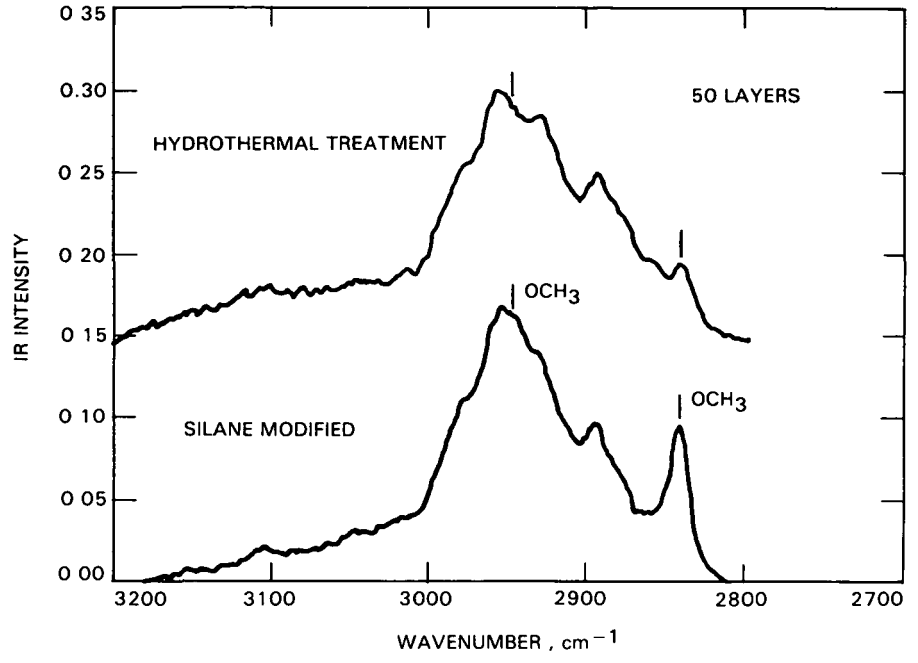

Figure 9. Spectra of γ-MPS on Sunadex Glass Before and After Hydrothermal Treatment Showing the Extensive Removal of the Silane with Water Exposure

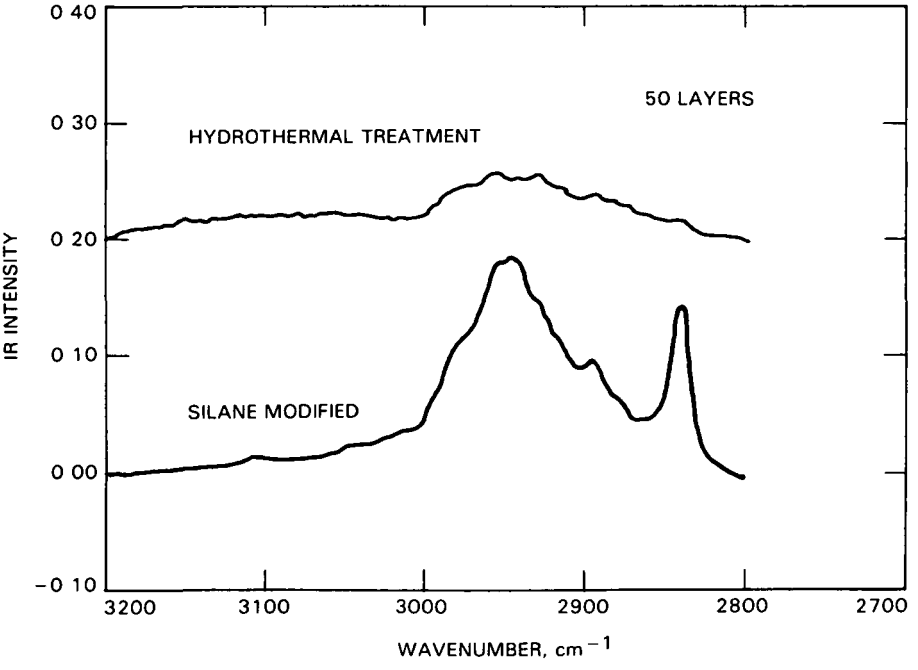

Figure 10. Spectra of γ-MPS on the Surface of Glass Spheres Which Have Been Acid-Washed to Prepare the Surface Prior to Treatment with the Silane. (The spectra are shown before and after hydrothermal treatment showing that the acid improves the stability.)

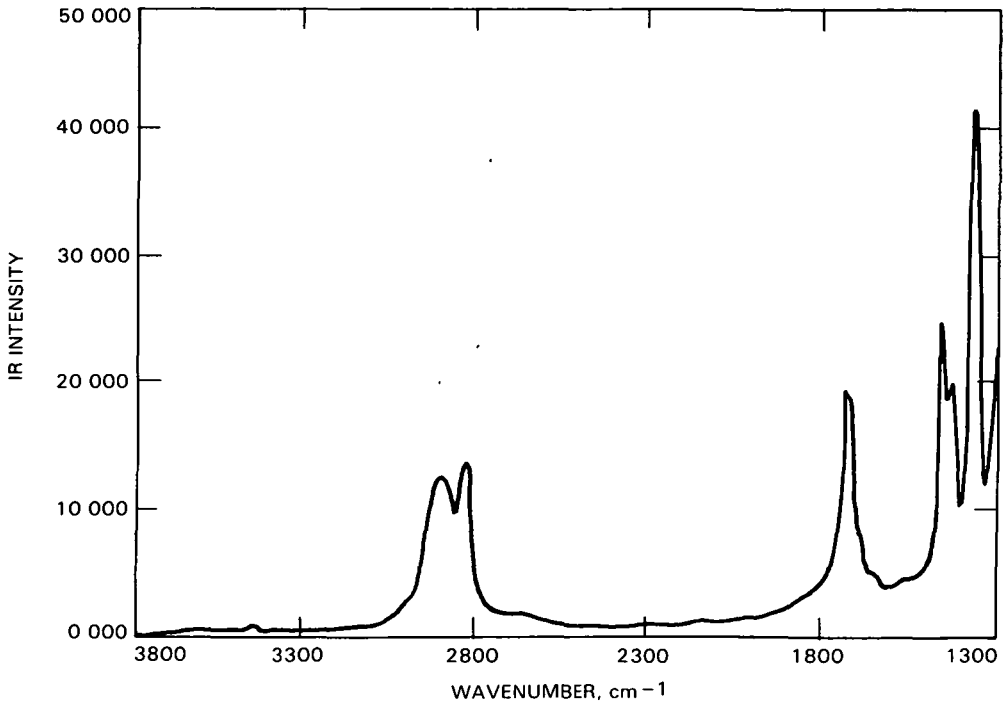

Figure 11. DRIFT Spectrum of Pure EVA

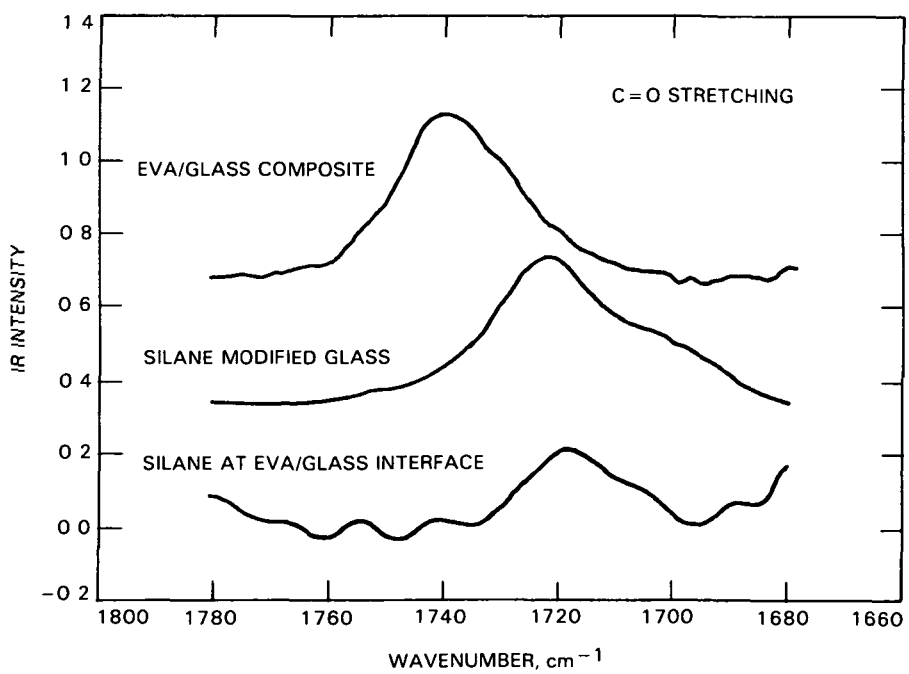

Figure 12. DRIFT Spectrum Showing the Silane at the EVA/Glass Interface. (The top spectrum is the EVA/glass spectrum, the middle spectrum is the spectrum of the Y-MPS modified glass, and the bottom is the difference spectrum obtained by subtracting the treated glass spectrum from the composite. The bands observed are associated with the interfacial silane structure.)

observed that structural changes occur as a result of the peroxide-induced polymerization of the coupling agent. This polymerization is indicated by the loss of the carbon-hydrogen stretching mode of the vinyl group as indicated in Figure 13. Quantitative determinations of the amount of Y-MPS polymerization can be made. The calculations indicate that nearly 80% of the Y-MPS has polymerized with the peroxide, and only 20% of the Y-MPS has polymerized in the absence of the peroxide. This polymerization of the Y-MPS produces an interlocking interpenetrating network with the EVA (see Figure 2). This interpenetrating network has nonhydrolyzable carbon-carbon bonds as well as the hydrolyzable Si-O-Si bonds. The presence of the carbon-carbon bonds should contribute to the hydrothermal stability of the EVA/glass interface.

D. HYDROTHERMAL AGING OF EVA/GLASS INTERFACE

Accelerated aging tests were performed by placing the model composites in water at 40, 60, and 80°C for lengths of time up to 5000 h at present. Samples were removed at specified times and tested mechanically according to specification ASTM D-638, and also tested by FTIR spectroscopy.

1. Mechanical Testing

For mechanical testing, the following properties were measured:

(1) Modulus (1% strain).

(2) Ultimate tensile strength.

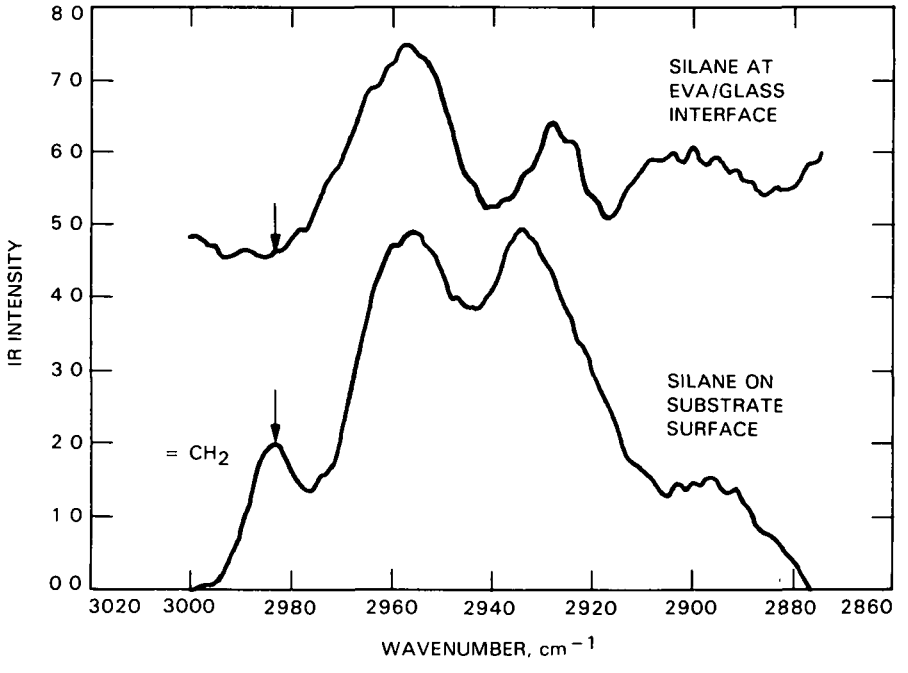

Figure 13. DRIFT Spectrum of Silane at the Interface Between Glass and EVA (Top Spectrum) and the Spectrum of the Y-MPS Silane of the Glass. (The top spectrum shows that the Y-MPS has polymerized during the formation of the interface because of the initiation by the peroxide.)

(3) Ultimate elongation.

(4) Dimensional change (length).

(5) Weight change (water absorption).

These measurements are tabulated for each temperature in Tables 3 through 5, and Tables 6 through 8 give the results for the test specimens dried at 105°C for a period of 72 h. The purpose for this was to determine the extent to which the bond strength was reversible by simply removing the absorbed water.

At 40°C water immersion (see Table 3), little effect was noticed for all the formulations except for 18181-A (EVA containing unprimed glass beads). This specimen slowly increased in water absorption from +0.15% weight gain after 100 h, to +51% weight gain after 2000 h. Apart from a minor decrease in elongation, the properties of this compound remained unchanged.

The 60°C water immersions (see Table 4) were found to be more severe, and then both the compounds with and without primer began to respond. The EVA without primer gained an enormous +2000% increase in weight at the 2000-h test point. The mechanical properties also shifted dramatically at this point and the compound lost 90% of its modulus, 96% of its tensile strength, and about 90% of its elongation. The equivalent compound with primed glass gained only +35% in weight; most of the other properties were only slightly affected. The equivalent polyethylene specimens gained only 3 to 4% water and were unaffected by the immersion. In the case of EVA, the difference between primed and unprimed glass filler is noticeable and suggests that the properties at the interface (adhesion bond) are responsible for the observed effects.

The next immersion temperature was 80°C (see Table 5) and resulted in rapid deterioration of the EVA specimens containing unprimed glass. After 500 h, the specimen had increased 500% in weight, and lost 80% of its tensile strength and elongation. Because of softening and tearing, this specimen did not survive the 1000-h immersion test point and was removed from further exposure. The EVA formulated with primer beads gained 61% by weight of water at the 1000-h test point and retained most of its other properties reasonably well. As with the previous experiments, the polyethylene compounds loaded with primed and unprimed glass beads showed only small gains from water absorption and were virtually unchanged.

It appears that the surface of the glass or the interface between the glass and the polymer is extremely hygroscopic and is effective in trapping large amounts of water in the polymer. The primer is of help in inhibiting this phenomenon and seems to give at least a ten-fold reduction in the amount of water absorbed. Water absorptions in the bulk polymer without fillers has been determined in a previous set of experiments (Reference 1). For EVA, the equilibrium water content at 40 and 60°C is on the order of +0.3%. At 80°C, pure EVA (Elvax 150) equilibrates at approximately 1% by weight water. These water absorption experiments indicate that the glass/polymer interface is the region affected.

A second set of test bars from the water immersion tests were dried to determine the extent of property recovery and give an indication as to when permanent and non-reversible damage had occurred. The results of these experiments are given in Tables 6 through 8. For the 40°C immersions, all the

Table 3. Hydrothermal Aging of Glass Bead-Filled Polymer Specimens at 40°C

Specimen	Property[a]	Control	100 h	500 h	2000 h
18181-A,	MOD	2830	1.6×10^3	1.7×10^3	8.3×10^2
EVA, Without	UT	1380	1295	1230	1210
Primer	UF, %	600	600	570	510
	Δwt %	--	+0.15%	+18.9%	+51%
	ΔL %	--	0	+5.5%	+15.3
18181-B,	MOD	2500	1.6×10^3	1.8×10^3	2.4×10^3
EVA, With	UT	905	1070	900	1150
Primer	UF, %	350	385	190	390
	Δwt %	--	+0.19%	+2%	+3.5%
	ΔL %	--	0	0	+1.3
18181-C,	MOD	8×10^4	1.2×10^5	1.2×10^5	1.2×10^5
Polyethylene,	UT	2180	1995	~2200	2360
Without	UF, %	~0	10	0	0
Primer	Δwt %	--	+0.52%	+1.4%	+2.5%
	ΔL %	--	0	0	0
18181-D,	MOD	1.6×10^5	1.7×10^5	1.6×10^5	1.5×10^5
Polyethylene,	UT	4340	4235	~4380	4490
With Primer	UF, %	20	10	0	0
	Δwt %	--	+0.31%	0	+0.6%
	ΔL %	--	0	0	0

[a]Mechanical properties by ASTM D-638, 10 in./minimum rate of strain, Δwt % = percent weight gain; ΔL % = percent length gain-tensile bar.

Table 4. Hydrothermal Aging of Glass Bead-Filled Polymer Specimens at 60°C

Specimen	Property[a]	Control	100 h	250 h	500 h	2000 h
18181-A,	MOD	2830	1.8×10^3	1.6×10^3	3.8×10^2	3×10^1
EVA, Without	UT	1380	1240	960	530	50
Primer	UF, %	600	570	515	300	60
	Δwt %	--	+0.92%	+29.3%	+410%	+2015%
	ΔL %	--	0	+10.8%	+78.4%	+179%
18181-B,	MOD	2500	2×10^3	2.5×10^3	2×10^3	1.6×10^3
EVA, With	UT	905	935	930	990	830
Primer	UF, %	350	445	285	315	120
	Δwt %	--	+0.36%	+4%	+6.3%	+34.7%
	ΔL %	--	0	0	+6%	+12.5%
18181-C,	MOD	8×10^4	1.1×10^5	1.4×10^5	1.1×10^5	3×10^4
Polyethylene,	UT	2,180	2230	2510	2070	2710
Without	UF, %	~0	5	~0	~0	~0
Primer	Δwt %	--	+0.6%	+1.4%	+2.5%	+4.8%
	ΔL %	--	0	0	0	0[b]
18181-D,	MOD	1.6×10^5	1.6×10^5	1.5×10^5	1.2×10^5	1.3×10^5
Polyethylene,	UT	4340	4400	4450	4270	2980
With Primer	UF, %	20	10	~0	~0	~0
	Δwt %	--	+0.33%	+0.7%	0	+3.08%
	ΔL %	--	0	0	0	0

[a]Mechanical properties by ASTM D-638, 10 in./minimum rate of strain, Δwt % = percent weight gain; ΔL % = percent length gain-tensile bar.

[b]Blistered appearance.

Table 5. Hydrothermal Aging of Glass Bead-Filled Polymer Specimens at 80°C

Specimen	Property[a]	Control	100 h	250 h	500 h	1000 h
18181-A,	MOD	2830	1.7×10^3	9.3×10^2	1.1×10^3	
EVA, Without	UT	1380	460	285	310	Removed[b]
Primer	UF, %	600	365	120	100	
	Δwt %	--	+17.4%	+568%	+503%	
	ΔL %	--	+26.7%	+109%	+96.2%	
18181-B,	MOD	2500	2.2×10^3	2.3×10^3	3×10^3	1.7×10^3
EVA, With	UT	905	987	1010	910	725
Primer	UF, %	350	275	245	220	140
	Δwt %	--	+1%	+12.9%	+16.9%	+61.7%
	ΔL %	--	0	+2.7%	+5.6%	+21.5%
18181-C,	MOD	8×10^4	1.2×10^5	1.3×10^5	1.3×10^5	1.2×10^5
Polyethylene,	UT	2180	2145	2160	2110	1930
Without	UF, %	~0	10	~0	~0	~0
Primer	Δwt %	--	+1.4%	+3.5%	+4.1%	+4.3%
	ΔL %	--	0	+0.2%	+0.4%	+0.6%
18181-D,	MOD	1.6×10^5	1.8×10^5	1.7×10^5	1.4×10^5	1.2×10^5
Polyethylene,	UT	4340	4445	3990	3610	2910
With Primer	UF, %	20	10	~0	~0	~0
	Δwt %	--	+0.43%	+0.7%	+2.9%	+4.5%
	ΔL %	--	0	0	+2.2%	+0.2%

[a]Mechanical properties by ASTM D-638, 10 in./minimum rate of strain, Δwt % = percent weight gain; ΔL % = percent length gain-tensile bar.

[b]Specimens too soft to be tested, break on handling.

Table 6. Effect of Drying Out[a] the Hydrothermally Aged Specimens Reported in Table 3

Specimen	Property[b]	Control	100 h	500 h	2000 h
18181-A, EVA, Without Primer	MOD	2.8×10^3	2.4×10^3	3.4×10^3	2.2×10^3
	UT	1380	1205	1280	1210
	UF, %	600	590	565	570
	Δwt %	--	--	--	--
	ΔL %	--	--	--	--
18181-B, EVA, With Primer	MOD	2.5×10^3	2.2×10^3	3×10^3	2.6×10^3
	UT	905	965	990	860
	UF, %	350	325	315	260
	Δwt %	--	--	--	--
	ΔL %	--	--	--	--
18181-C, Polyethylene, Without Primer	MOD	8×10^4	1.8×10^5	1.6×10^5	1.5×10^5
	UT	2180	2790	1770	3710
	UF, %	0	~0	~0	~0
	Δwt %	--	--	--	--
	ΔL %	--	--	--	--
18181-D, Polyethylene, With Primer	MOD	1.6×10^5	1.8×10^5	1.6×10^5	1.7×10^5
	UT	4340	4720	4571	4380
	UF, %	20	~0	~0	~0
	Δwt %	--	--	--	--
	ΔL %	--	--	--	--

[a]Dried in circulating air oven, 105°C, 72 h.

[b]Mechanical properties by ASTM D-638, 10 in./minimum rate of strain, Δwt % = percent weight gain; ΔL % = percent length gain-tensile bar.

Table 7. Effect of Drying Out[a] the Hydrothermally Aged Specimens Reported in Table 4

Specimen	Property[b]	Control	100 h	250 h	500 h	2000 h
18181-A, EVA, Without Primer	MOD	2.8×10^3	2.5×10^3	3×10^3	2.7×10^3	1.1×10^3
	UT	1380	1270	1340	960	480
	UF, %	600	590	575	500	280
	Δwt %	--	--	--	--	--
	ΔL %	--	--	--	--	--
18181-B, EVA, With Primer	MOD	2.5×10^3	2.6×10^3	3.1×10^3	3.1×10^3	2.8×10^3
	UT	905	955	890	980	850
	UF, %	350	290	240	240	240
	Δwt %	--	--	--	--	--
	ΔL %	--	--	--	--	--
18181-C, Polyethylene, Without Primer	MOD	8×10^4	1.6×10^5	1.7×10^5	1.8×10^5	1.8×10^5
	UT	2180	2580	3680	3050	2680
	UF, %	0	~0	~0	~0	0
	Δwt %	--	--	--	--	--
	ΔL %	--	--	--	--	--
18181-D, Polyethylene, With Primer	MOD	1.6×10^5	1.9×10^5	1.8×10^5	1.4×10^5	1.6×10^5
	UT	4340	4530	4890	4510	3590
	UF, %	20	~0	~0	~0	0
	Δwt %	--	--	--	--	--
	ΔL %	--	--	--	--	--

[a]Dried in circulating air oven, 105°C, 72 h.

[b]Mechanical properties by ASTM D-638, 10 in./minimum rate of strain, Δwt % = percent weight gain; ΔL % = percent length gain-tensile bar.

Table 8. Effect of Drying Out[a] the Hydrothermally Aged Specimens Reported in Table 5

Specimen	Property[b]	Control	100 h	250 h	500 h	2000 h
18181-A, EVA, Without Primer	MOD	2.8×10^3	2.7×10^3	1.8×10^3		
	UT	1380	1175	560	(see footnote c)	
	UF, %	600	545	290		
	Δwt %	--	--	--		
	ΔL %	--	--	--		
18181-B, EVA, With Primer	MOD	2.5×10^3	2.6×10^3	2.6×10^3	2.8×10^3	2.6×10^3
	UT	905	905	920	1020	880
	UF, %	350	240	310	405	260
	Δwt %	--	--	--	--	--
	ΔL %	--	--	--	--	--
18181-C, Polyethylene, Without Primer	MOD	8×10^4	1.4×10^5	1.8×10^5	1.7×10^5	1.8×10^5
	UT	2180	3160	3280	2440	3010
	UF, %	0	~0	~0	~0	~0
	Δwt %	--	--	--	--	--
	ΔL %	--	--	--	--	--
18181-D, Polyethylene, With Primer	MOD	1.6×10^5	1.6×10^5	1.5×10^5	1.6×10^5	1.8×10^5
	UT	4340	4415	4100	3800	3710
	UF, %	20	~0	~0	~0	~0
	Δwt %	--	--	--	--	--
	ΔL %	--	--	--	--	--

[a]Dried in circulating air oven, 105°C, 72 h.

[b]Mechanical properties by ASTM D-638, 10 in./minimum rate of strain, Δwt % = percent weight gain; ΔL % = percent length gain-tensile bar.

[c]Broken, removed from further testing.

specimens recovered almost all their original properties. At 60°C, signs of permanent damage now became apparent in the EVA specimen filled with unprimed glass beads. At the 500-h point, the tensile strength decreased by 30%, and at the 2000-h point, it had decreased to 65% of control. About a 50% reduction of elongation at break was also found at this point. The other EVA compound containing primed glass recovered most of its control properties upon drying. The 80°C test specimens gave much the same performance except that now non-reversible effects seem to start at after about 250 h in the unprimed EVA/glass specimen. Primed EVA/glass specimens survived 2000 h at this temperature without damage.

2. Spectroscopic Testing

As reported in the previous section, the mechanical properties as a function of hydrothermal aging of the EVA composites without primer had substantial declines, whereas when the glass surface is treated with the primer solution, the composites show a remarkable resistance to loss of mechanical properties, as a function of hydrothermal aging time and temperature.

An additional result of the accelerated hydrothermal aging is the incorporation of water into the composite structure, generally absorbing water to many times their original weight.

For chemical information using FTIR spectroscopy, a preliminary experiment was carried out involving an accelerated hydrothermal aging of an EVA/glass composite. The test consisted of an 85°C water treatment for 2 months with subsequent drying at 100°C in vacuum. The FTIR spectra of the sample over the region 2200 to 3800 cm^{-1} before and after the hydrothermal treatment are shown in Figure 14. No major chemical differences were observed except for the apparent uptake of water which was not removed in spite of the rather substantial drying. This water is presumed to be on the surface of the glass powder as it is well known that the interface is the preferred site of the sorbed water. Examination of the spectra of the hydrothermally treated sample in other spectral regions showed no observable chemical degradation after 2 months. The primed EVA/glass interface has resisted hydrothermal attack up to at least 2 months (1440 h) of accelerated testing. This represents extraordinary stability.

The EVA/glass composites (which had undergone up to 2000 h of hydrothermal aging in water at 60°C, and whose aging properties are shown in Table 4) were also examined by FTIR spectroscopy. The FTIR spectra of these samples after 100, 250, 500, and 2000 h are shown in Figure 15, over the region 3500 to 4000 cm^{-1}. Up to 500 h, FTIR spectroscopy of this sample found no evidence for chemical changes and, as with the preliminary sample, detected only water uptake.

However, at 2000 h of hydrothermal aging, a new infrared band occurred at 3680 cm^{-1} [see Figure 15(D)]. With this finding, the FTIR spectra of the unprimed EVA/glass composites which had been hydrothermally aged at 60°C were taken to serve as comparative controls. Again, after 2000 h of aging, this new band at 3680 cm^{-1} was observed, and it was tentatively concluded that this was not related to the primer. Examination of the mechanical property data in Table 4 for the primed EVA/glass specimen hints at changes (after 2000 h) that

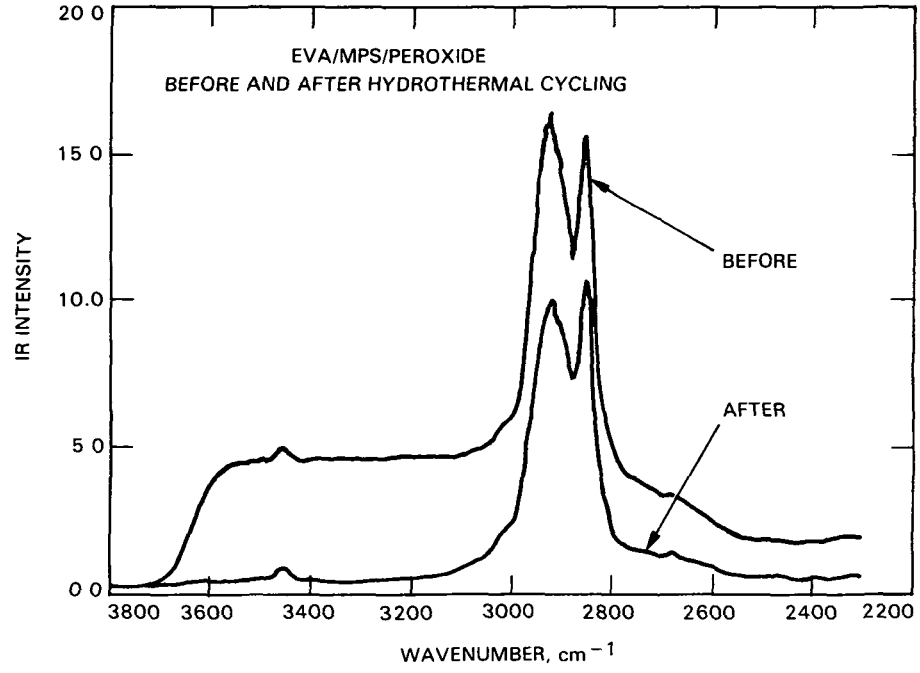

Figure 14. DRIFT Spectrum of the EVA/γ-MPS-Peroxide Before and After Hydrothermal Cycling. (The uptake of water is shown by the increase in the absorption between 3610 and 3200 cm^{1}.)

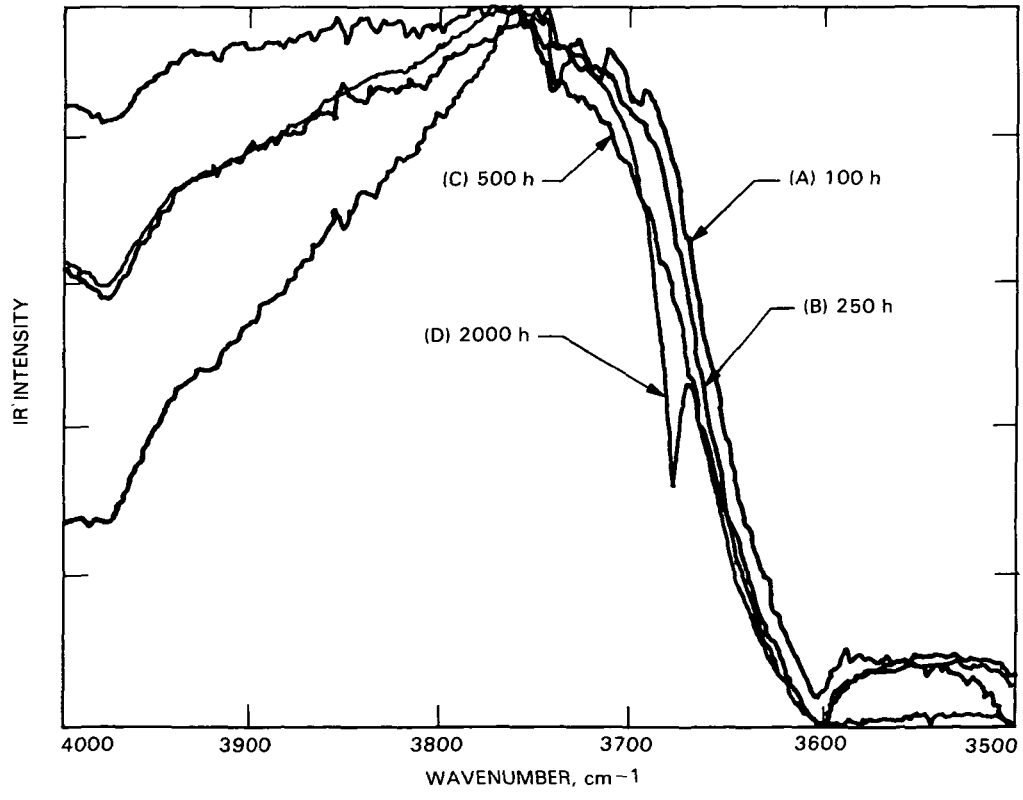

Figure 15. FTIR Spectra of Primed EVA/Glass Bead Specimens, Hydrothermally Aged at 60°C

seem to be outside the data patterns observed for lower aging times. It is tempting to interpret this band as spectroscopic evidence of some irreversible interfacial event related to hydrothermal attack, although assignment of this band to a given chemical reaction is not clear at this time.

SECTION III

CHEMICAL BONDING BETWEEN SOLAR CELLS AND EVA

Ethylene/vinyl acetate (EVA) has been developed for use as an encapsulation material for photovoltaic devices. However, there are two important problems associated with the use of EVA in such applications: (1) the adhesion of EVA to the aluminized rear surface of silicon cells is poor, especially during exposure to moisture or high relative humidities at elevated temperatures; and (2) most tests (such as the peel test) that are used to evaluate the adhesion are destructive in nature. Such tests provide little information about the onset of delamination processes and about the likely lifetime of a bonded assembly.

The initial phase of this research had two primary objectives: (1) to investigate the use of silane coupling agents as primers to enhance the hydrothermal stability of adhesive bonds between EVA and aluminum, and (2) to develop non-destructive optical techniques for determining the stability of polymer/metal interfaces during exposure to moisture at elevated temperatures. Toward this end, qualitative tests were carried out investigating the adhesion of EVA to several types of aluminum substrates, which included vapor-deposited aluminum mirrors on glass, and the aluminized back surfaces of commercial solar cells. The results obtained are described below.

A. ALUMINUM MIRRORS

Adhesive bonding between EVA and most aluminum surfaces without primers are weak and are weakened even further by exposure to warm water. The hydrothermal stability of the EVA/aluminum interface is improved by the use of silane primers.

For studies with aluminum mirrors, reflection-absorption infrared (RAIR) spectroscopy has been used to determine the nature of the interface between Y-MPS and the oxidized surface of aluminum. RAIR is a technique for obtaining infrared spectra of thin films on metal substrates by reflecting infrared radiation polarized parallel to the plane of incidence off the metals at large, almost grazing angles. RAIR spectra obtained from Y-MPS films deposited on aluminum mirrors from dilute methanol solutions were always characterized by absorption bands near 1720 and 1100 cm^{-1} that were assigned to carbonyl and siloxane groups (Figure 16), regardless of the concentration of the solutions. However, spectra obtained from Y-MPS films that were deposited from methanol solutions, and then rinsed with methanol, were characterized by bands near 1700 and 930 cm^{-1} (Figure 17). The band near 1700 cm^{-1} was assigned to carbonyl groups that were hydrogen bonded to surface hydroxyl groups. The band near 930 cm^{-1} was assigned to silanol groups that were also hydrogen bonded to the substrate. It seems that the first layer of Y-MPS molecules is absorbed onto aluminum by hydrogen bonding through both the silanol and carbonyl groups. This may help to explain the effectiveness of Y-MPS as a primer for enhancing the hydrothermal stability of adhesive bonds between EVA and substrates such as aluminum. If the first layer of Y-MPS is absorbed through two functional groups, it may be more difficult to displace from the surface than if it was absorbed only through, for instance, the silanol groups.

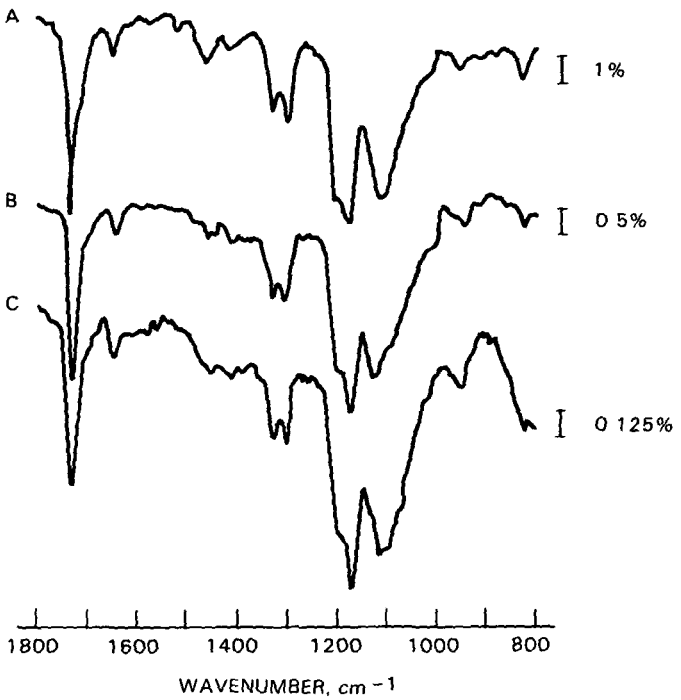

Figure 16. Infrared Spectra of Y-MPS Films with Three Different Thicknesses Deposited on Aluminum Mirrors

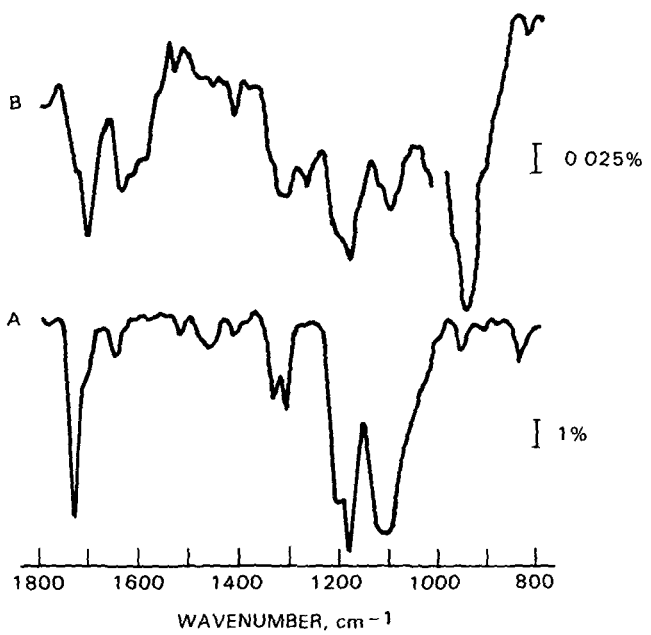

Figure 17. Infrared Spectra of: (A) Thick, and (B) Thin (Monolayer) Films of Y-MPS on Aluminum Mirrors

Another important result obtained during the first phase of this research with aluminum mirrors was the development of ellipsometry as a non-destructive probe for monitoring the polymer/metal interface during exposure to an aggressive environment such as warm water. This technique involves the use of an optical ellipsometer to measure the relative amplitude reduction (called ψ), and the relative phase shift (called Δ) for the parallel and perpendicular components of linearly polarized light reflected from a polymer-coated metal substrate that is immersed in warm water.

Results obtained for an uncoated aluminum mirror that was evaporated onto a glass slide and then immersed in water at 40°C indicated that Δ initially decreased by several degrees before increasing somewhat, and then decreased again (Figure 18). The first decrease in Δ was interpreted as the dissolution of the native oxide, and the second decrease indicated reprecipitation of the hydroxide known as pseudoboehmite on the aluminum surface.

The conversion of the native oxide on aluminum to the hydrated oxide pseudoboehmite is generally considered to be the cause of debonding of polymers from aluminum in the presence of warm water (Reference 20). In order to obtain stable bonds between a rubbery polymer such as EVA and aluminum, it is necessary to inhibit that corrosion. These preliminary tests with uncoated aluminum mirrors demonstrated that the corrosion reaction could be followed by RAIR and also by ellipsometry. The next series of experiments were intended to learn if these same techniques could monitor the corrosion reaction through a coating of EVA.

B. ALUMINUM MIRRORS WITH EVA COATINGS

When a thin film of EVA containing the cross-linking agent Lupersol 101 was laminated onto an unprimed, vapor-deposited aluminum mirror and then immersed in warm water, ellipsometry results similar to those shown in Figure 19 were obtained. An induction period lasting approximately 10 h was observed during which Δ changed very little. Thereafter, Δ increased slowly, but steadily. When a thin film of A-11861 primer was applied to the aluminum substrate before the substrate was laminated with EVA, the ellipsometry results were similar, but the rate of increase of Δ as a function of time after the induction period was considerably lower.

When a thin film of EVA containing the cross-linking agent TBEC was laminated onto an aluminum film that had been evaporated onto a glass slide and then immersed in warm water, the ellipsometry results were quite different. In that case, almost no induction period was observed. Instead, Δ began to rise almost immediately (Figure 20).

These results were interpreted as follows:

(1) When EVA is cross-linked with Lupersol 101, the reaction proceeds mostly through the vinyl acetate groups.

(2) The ethylene units are relatively unaffected and remain in rather crystalline regions.

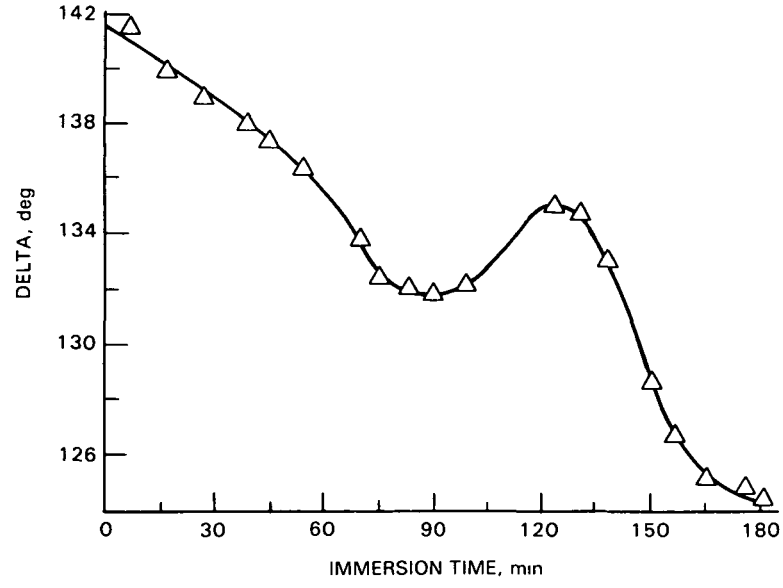

Figure 18. Ellipsometry Parameter Δ Versus Immersion Time in Water at 40°C for an Uncoated Aluminum Mirror

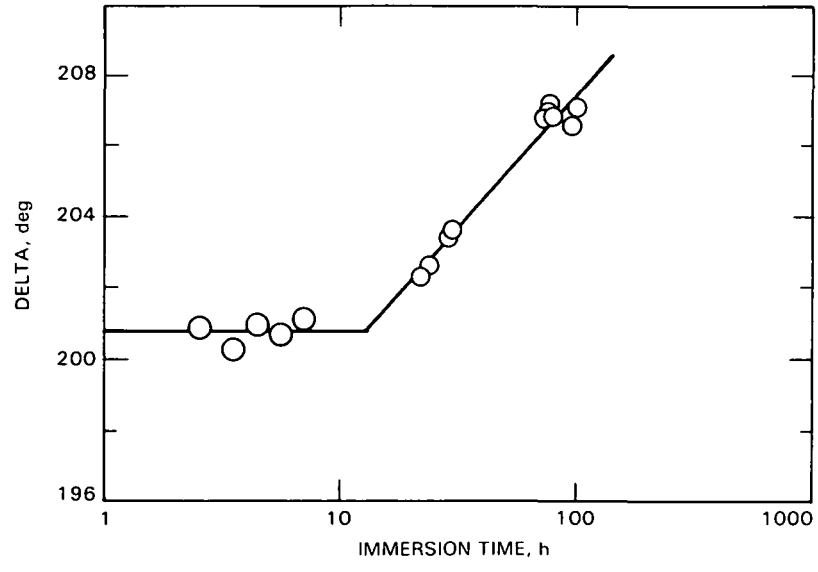

Figure 19. Ellipsometry Parameter Δ Versus Immersion Time in Water at 40°C for EVA Cured with Lupersol 101 Laminated on Vapor-Deposited Aluminum

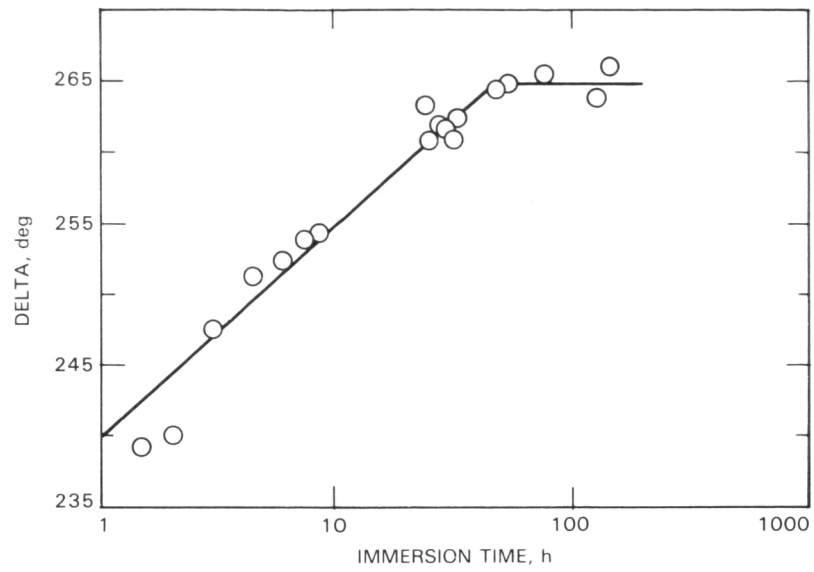

Figure 20. Ellipsometry Parameter Δ Versus Immersion Time in Water at 40°C for EVA Cured with TBEC Laminated on Vapor-Deposited Aluminum

(3) Water does not diffuse through these crystalline regions very quickly and a substantial induction period is observed before water reaches the aluminum surface.

(4) Once water reaches the surface, dissolution of the native oxide and reprecipitation of pseudoboehmite begin.

(5) The arrival of water at the interface and the precipitation of pseudoboehmite both cause the parameter Δ to rise.

When EVA is cross-linked with TBEC, cross-linking occurs through both the ethylene and vinyl acetate groups. In this case, there are no crystalline ethylene regions and the diffusion of water to the interface is fast. The ellipsometry parameter Δ rises quickly during exposure to water at elevated temperatures.

Independent of the choice of cross-linking agent, these experiments nevertheless demonstrated that the moisture-induced corrosion of the surfaces of aluminum mirrors could be detected by ellipsometry through a coating of cross-linked EVA. In addition, there was some evidence that γ-MPS slowed, but did not stop the corrosion of these aluminum mirrors.

C. ALUMINIZED SOLAR CELLS

Two different kinds of aluminized back surfaces have been identified using scanning electron microscopy. Both kinds are quite rough, but there are significant differences in their morphologies. The first type of aluminized

back surface consists of ridges separated by channels (Figure 21). Analysis of such surfaces by energy dispersive x-ray analysis (EDAX) showed that they contained a great deal of silicon as well as aluminum. Generally speaking, the ridges were rich in silicon and the channels were rich in aluminum (Figure 22). These solar cells with a back surface mixture of aluminum and silicon were designated "type 1" solar cells.

Auger electron spectroscopy (AES) was also used to characterize the back surfaces of "type 1" cells. Auger spectroscopy is much more surface sensitive than EDAX, but the results were similar. Silicon Auger bands were observed near 78 and 92 eV (Figure 23). The band near 78 eV is characteristic of silicon in an oxide and the band near 92 eV is indicative of elemental silicon. The aluminum AES bands were observed near 53 and 64 eV. These bands are characteristic of aluminum in the oxidized and elemental states, respectively.

The second type of aluminized back surface solar cells, designated as "type 2," was characterized by large numbers of small, irregularly shaped features (Figure 24). X-ray photoelectron spectra (XPS) of such surfaces were characterized by bands near 74, 124, 285, and 531 eV (Figure 25). The XPS bands near 74 and 124 eV were assigned to aluminum in an oxidized state, and the XPS band near 531 eV was assigned to oxygen in an oxide, indicating that the back surface of "type 2" cells was mostly composed of an aluminum oxide. The XPS band near 531 eV was assigned to carbon in absorbed hydrocarbons. There was essentially no silicon on the back surface of "type 2" cells.

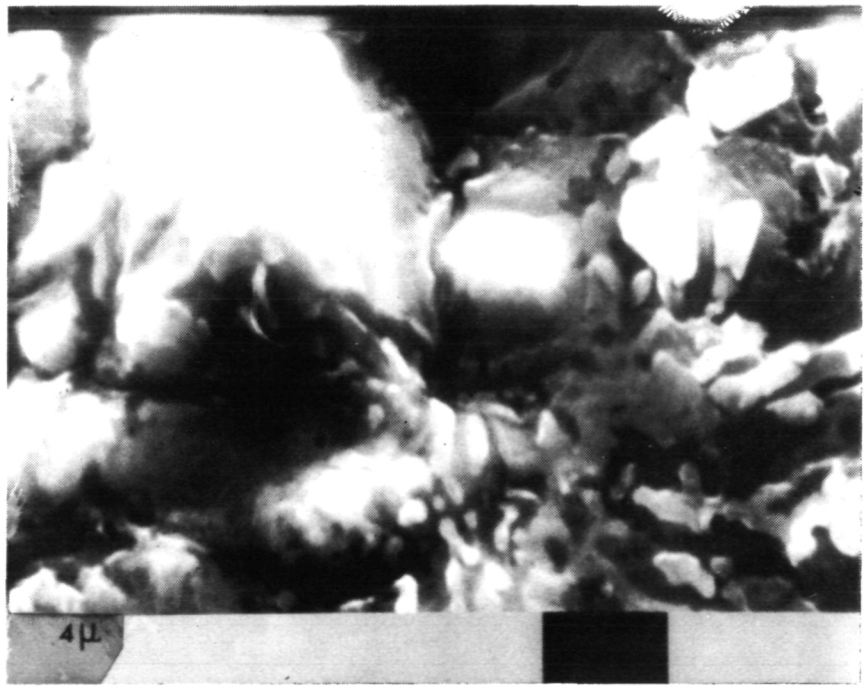

Figure 21. Scanning Electron Micrograph of Back Side of "Type 1" Silicon Cell (5000X)

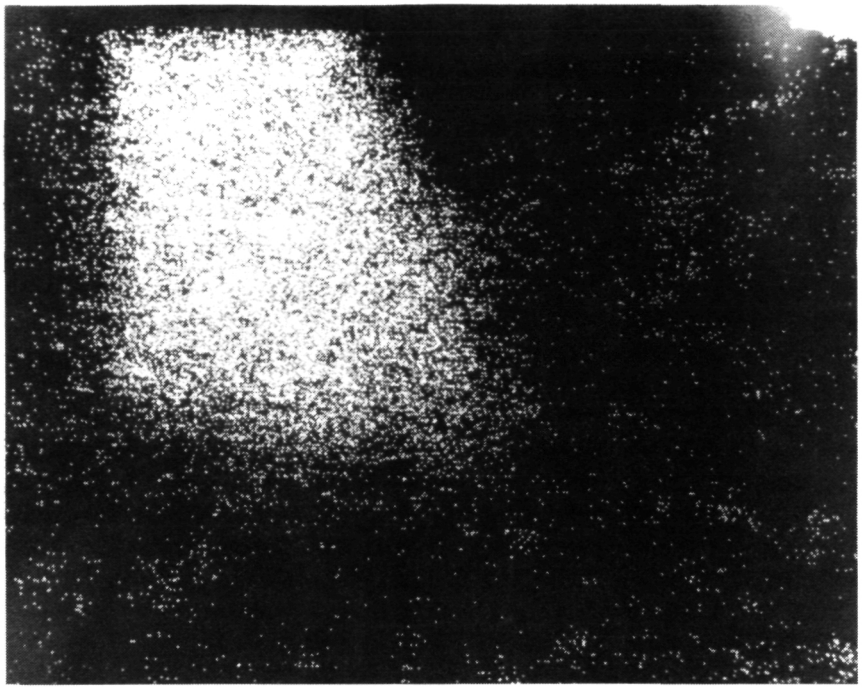

(A)

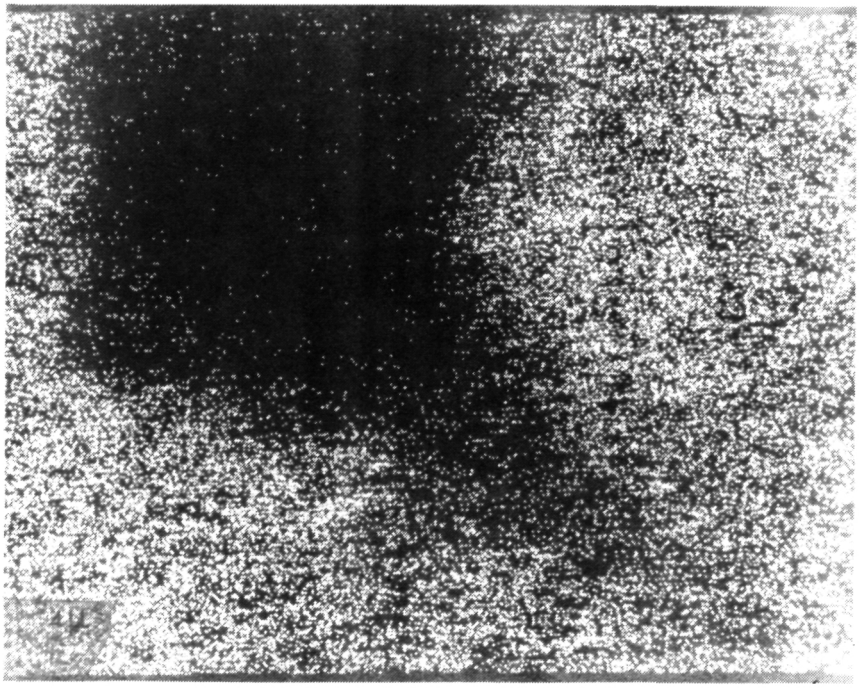

(B)

Figure 22. EDAX: (A) Silicon and (B) Al Maps of Back Side of Same Silicon Cell as in Figure 21

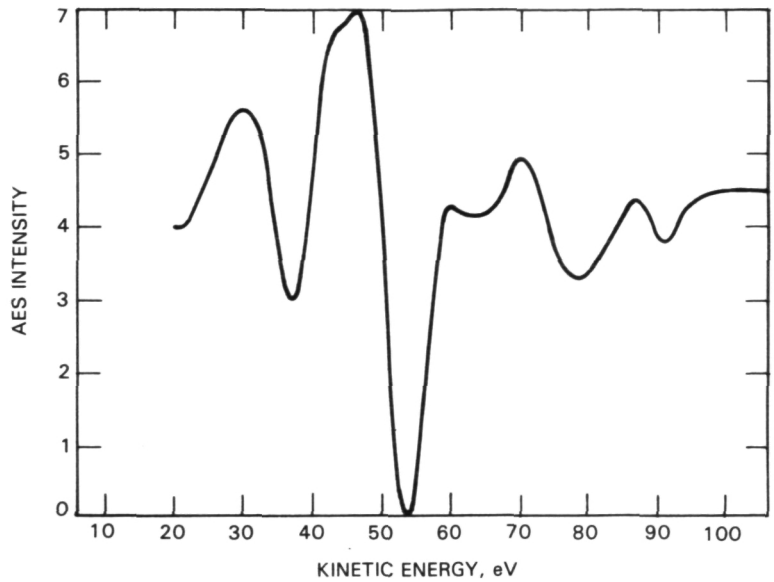

Figure 23. Auger Electron Spectra of Back Side of Same Silicon Cell as in Figure 21

Figure 24. Scanning Electron Micrograph of Back Side of "Type 2" Silicon Cell (2000X)

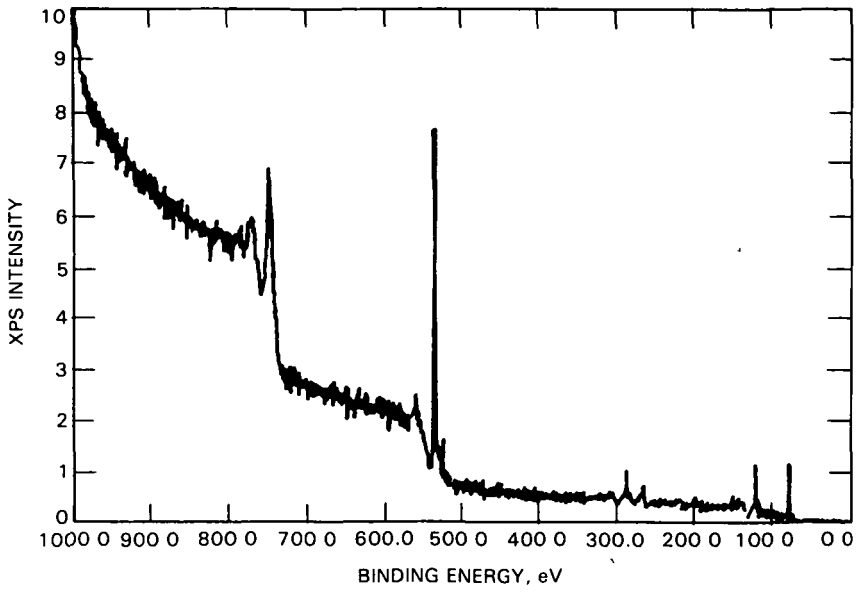

Figure 25. X-ray Photoelectron Spectrum of Back Side of As-Received "Type 2" Silicon Cell

Several different investigations were carried out to determine the failure mechanisms for adhesive bonds between EVA and the aluminized back surfaces of silicon cells. In one experiment, an EVA film was laminated onto an unprimed "type 2" cell and then peeled off. The adhesion of the film to the cell was very good and it was very difficult to peel the film. XPS spectra, obtained from the cell after the EVA film had been peeled off, were characterized by a strong band near 285 eV that was assigned to carbon (Figure 26). However, there was very little evidence of aluminum, indicating that the failure of the bond was cohesive within the EVA. In a repeat experiment, EVA was laminated onto the backside of an unprimed "type 2" cell and the cell was then boiled in water for 1 h. Once again, it was very difficult to peel the EVA from the cell, indicating that the adhesion of the film to the cell was still quite good. However, some evidence for aluminum was observed in the XPS spectra obtained from the cells, showing that the locus of failure between EVA and aluminum was closer to the interface after boiling in water (Figure 27), presumably because of the formation of pseudoboehmite.

The tests just described were destructive in nature and, as indicated earlier, the program intent is to develop non-destructive tests. Therefore, the application of optical techniques (such as ellipsometry and reflection-absorption infrared spectroscopy) for the non-destructive characterization of adhesive bonds between EVA, and the aluminized back surface of silicon cells have been investigated.

It was determined, however, that ellipsometry was not suitable for use on the back surfaces of the cells. These surfaces were much rougher than the surfaces of aluminum mirrors and, therefore, accurate ellipsometry data could not be obtained. As a result, we have concentrated on the use of infrared

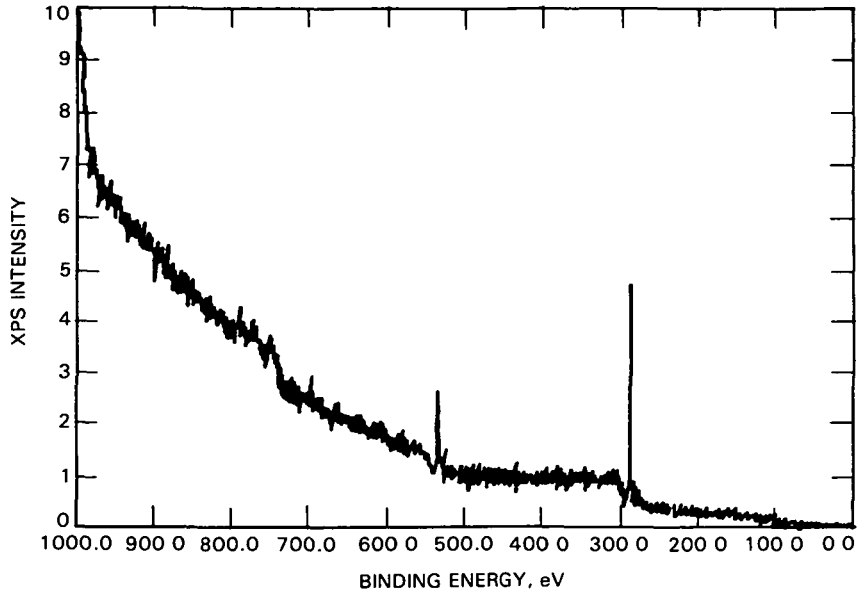

Figure 26. XPS Spectrum of Laminated "Type 2" Silicon Cell After Peeling EVA Film

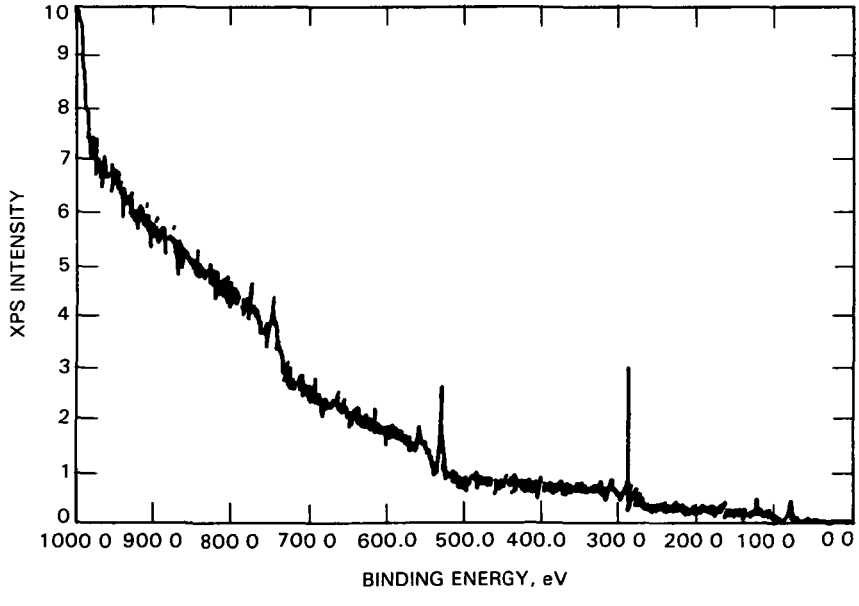

Figure 27. XPS Spectrum of Laminated "Type 2" Silicon Cell After Boiling 1 h and Peeling EVA Film

spectroscopy for the non-destructive characterization of the interface between EVA and the backside of silicon cells. Trial experimentation indicated that "type 1" solar cells were a better choice for RAIR examination because of much higher specular infrared reflectivity.

D. REFLECTION ABSORPTION INFRARED SPECTROSCOPY STUDIES

As described earlier, the failure mechanism of adhesive bonds to aluminum mirrors usually involves the conversion of the native oxide to the hydrated oxide known as pseudoboehmite (Reference 20) and, initially, it was desired to determine if exposure of solar cells to water at elevated temperatures also resulted in the formation of pseudoboehmite on the back surfaces of these cells. Infrared spectra was obtained from the backside of a "type 1" cell before and after the cell was boiled in water for 1 h. The results are shown in Figure 28. The spectrum obtained from the cell before boiling was essentially flat and featureless, but the spectrum obtained after boiling was characterized by a strong band near 1080 cm^{-1} that was indicative of pseudoboehmite.

Next, it was desired to determine if the formation of pseudoboehmite beneath a film of EVA could be detected by RAIR. Accordingly, the infrared spectrum was obtained of a "type 1" cell that was boiled in water for 30 min and then coated with a thin film of uncrosslinked EVA that was several hundreds of angstroms in thickness (Figure 29). Strong bands characteristic of EVA were easily observed near 1740 and 1255 cm^{-1}, but the band near 1080 cm^{-1} that is characteristic of pseudoboehmite was also observed. These results showed that pseudoboehmite could be detected beneath EVA films on silicon cells.

Next, a thin film of uncrosslinked EVA was applied to a "type 1" cell and the cell was then boiled in water. Occasionally, the cell was removed from the water and examined by infrared spectroscopy. The results obtained are shown in Figure 30. Initially, only the bands characteristic of EVA were observed near 1740 and 1255 cm^{-1}. However, after immersion of the cell in boiling water for 20 min, some changes were observed in the infrared spectra and, after 50 min, the band characteristic of pseudoboehmite was clearly observed near 1080 cm^{-1}.

In another series of experiments, infrared spectroscopy was used to determine the effects of a cross-linked coating of EVA with and without primer A-11861 on the aluminized back surfaces of silicon cells. For the first test without primer, a thin film of EVA was applied to a "type 1" cell by dipping the cell in a 0.25% solution of EVA in chloroform. The film was then cross-linked using Lupersol 101 and the cell was immersed in boiling water. The cell was removed from the water at intervals of 30 min and examined using infrared spectroscopy. Initially, only bands characteristic of EVA were observed, but after 30 min, the band characteristic of pseudoboehmite was clearly observed near 1080 cm^{-1} (Figure 31). After 60 min, the band near 1080 cm^{-1} was quite strong, indicating that hydration of the aluminum oxide beneath the EVA film was very rapid. Cross-linking of the EVA alone did not stop the formation of the pseudoboehmite.

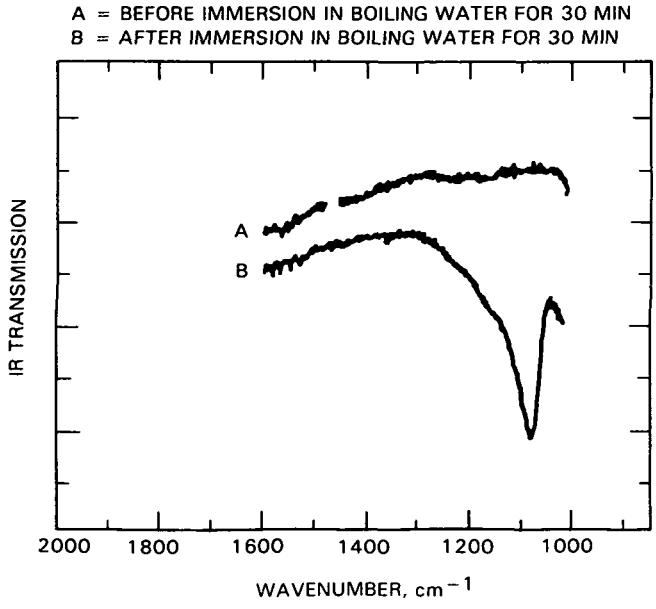

Figure 28. Reflection Infrared Spectra Obtained from Aluminized Back Side of "Type 1" Silicon Cell

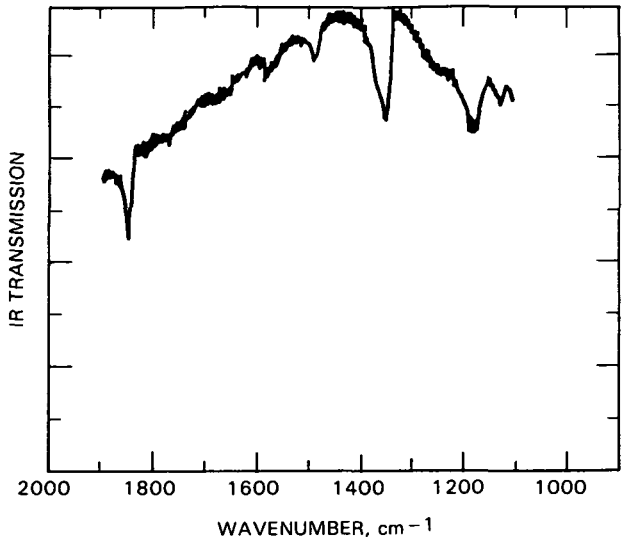

Figure 29. Reflection Infrared Spectrum Obtained from Aluminized Back Side of "Type 1" Silicon Cell, Boiled in Water for 30 min, and Then Coated with a Thin Film of EVA

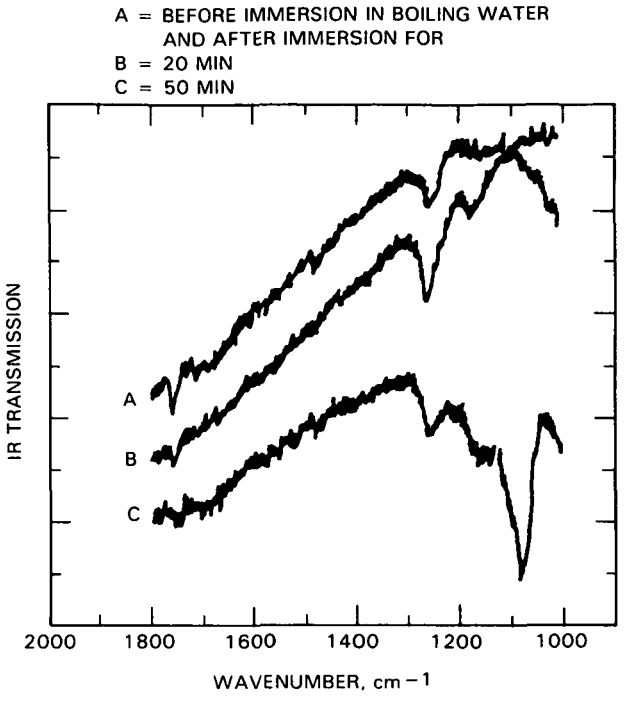

Figure 30. Reflection Infrared Spectra Obtained from Aluminized Back Side of a "Type 1" Silicon Cell Coated with a Thin Film of EVA

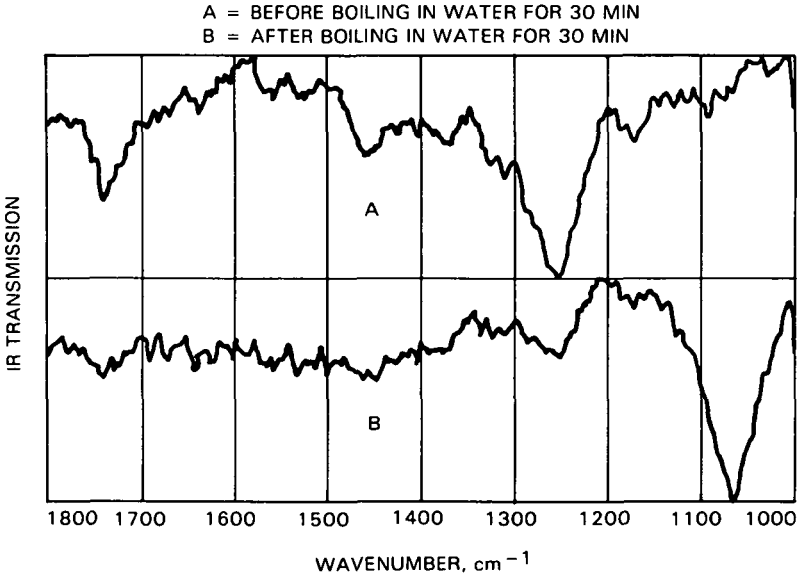

Figure 31. Reflection Infrared Spectra Obtained from the Back Side of a "Type 1" Silicon Cell Coated with a Thin Film of EVA, But No Primer

Finally, the experiment just described was repeated, except that a thin film of primer A-11861 was applied to the backside of the cell before the EVA film was applied and cross-linked. The initial spectra of the cell were similar to those of the unprimed cell, except that some bands characteristic of the primer were observed between 1200 and 1000 cm^{-1} [Figure 32(A)]. However, the band near 1080 cm^{-1} was not observed even after the cell was immersed in boiling water for times as long as 90 min [Figure 32(B)], and it was concluded that the primer inhibited the formation of pseudoboehmite on the aluminized back surfaces of "type 1" solar cells. This result is in dramatic contrast to the behavior of aluminum mirrors, where EVA and the Y-MPS-based primer was not effective to stop pseudoboehmite formation. Although unexplained at this time, the possibilities of a self-priming EVA for both glass and solar cells using a common primer is strongly indicated.

The results obtained thus far can be summarized as follows. The adhesion of EVA to the oxidized surfaces of smooth metals is marginal, but is improved by the use of primers containing silane coupling agents such as Y-MPS. Ellipsometry is an excellent in-situ, non-destructive technique for monitoring the stability of interfaces between EVA and smooth, reflecting metals. The aluminized back surfaces of silicon cells are very rough and porous. The adhesion of EVA to such surfaces is excellent, especially when primers containing Y-MPS are used. Failure of adhesive bonds between EVA and the aluminized back surface of silicon cells during exposure to moisture at elevated temperatures involves the transformation of the native oxide to the hydrated oxide known as pseudoboehmite. Ellipsometry cannot be used to follow the formation of pseudoboehmite on the back surfaces of such cells because of their poor reflectivity. However, infrared spectroscopy can be used to determine the formation of pseudoboehmite under EVA films on the back surfaces of silicon cells.

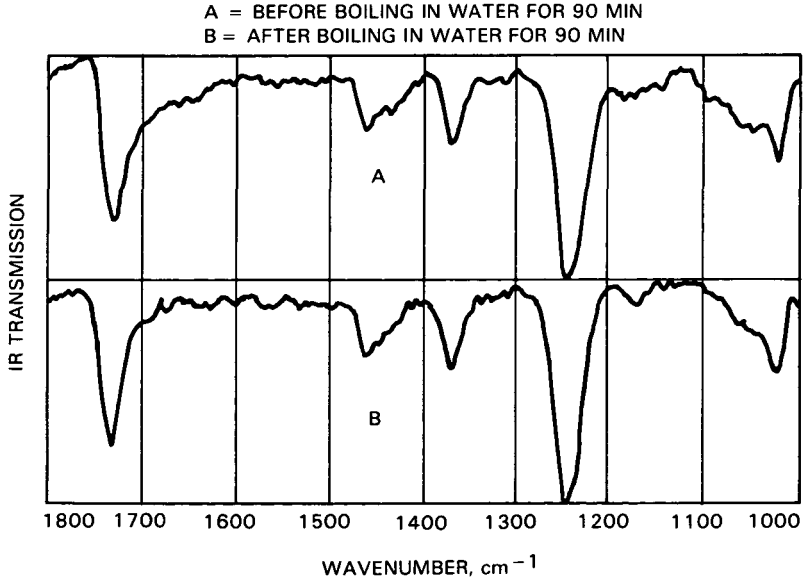

Figure 32. Reflection Infrared Spectra Obtained from the Back Side of a "Type 1" Silicon Cell Coated with Thin Films of A-11861 Primer and EVA

SECTION IV

REFERENCES

1. Willis, P.B., Investigation of Test Methods, Material Properties, and Processes for Solar Cell Encapsulants, Eighth Annual Report, DOE/JPL-954527-84/27, Springborn Laboratories, Inc., Enfield, Connecticut, July 1984.

2. Willis, P.B., Investigation of Test Methods, Material Properties, and Processes for Solar Cell Encapsulants, Ninth Annual Report, DOE/JPL-954527-85/28, Springborn Laboratories, Inc., Enfield, Connecticut, July 1985.

3. White, M.L., "Encapsulation of Integrated Circuits," Proceedings of the IEEE, Vol. 57, p. 1610, 1969.

4. Jaffe, D., "Encapsulation of Integrated Circuits Containing Beam Leaded Devices with a Silicone RTV Dispersion," IEEE Transactions on Parts, Hybrids, and Packaging, Vol. PHP 12, p. 182, 1976.

5. White, M.L., "Encapsulating Integrated Circuits," Bell Laboratories Record, p. 80, March 1974.

6. Shar, N.L., and Feinstein, L.G., "Performance of New Copper-Based Metallization Systems in an 85°C, 80% RH, Cl_2 Contaminated Environment," Proceedings of 1977 Electronic Components Conference, pp. 84-95, 1977.

7. Plueddemann, E.P., Chemical Bonding Technology for Terrestrial Solar Cell Modules, JPL 5101-132, Jet Propulsion Laboratory, Pasadena, California, September 1, 1979.

8. Coulter, D.R., Cuddihy, E.F., and Plueddeman, E.P., Chemical Bonding Technology for Terrestrial Photovoltaic Modules, JPL Publication 83-86, Jet Propulsion Laboratory, Pasadena, California, November 15, 1983.

9. Hair, M.L., Infrared Spectroscopy in Surface Chemistry, Marcel Dekker, Inc., New York, 1967.

10. Little, L.H., Infrared Spectra of Absorbed Species, Academic Press, London, 1966.

11. Ishida, H., and Koenig, J.L., J. Coll. and Inter. Sci., Vol. 64, p. 555, 1978.

12. Chiang, C.H., and Koenig, J.L., J. Polym. Sci., Polym. Phys. Ed., Vol. 20, p. 2135, 1982.

13. Graf, R.T., Koenig, J.L., and Ishida, H., J. Adhesion, Vol. 16, p. 97, 1983.

14. Graf, R.T., Koenig, J.L., and Ishida, H., Anal. Chem., Vol. 56, p. 773, 1984.

15. Culler, S.R., Ishida, H., and Koenig, J.L., The Use of Infrared Methods to Study Polymer Interfaces, Ann. Rev. Mater. Sci., Vol. 13, p. 363, 1983.

16. Kortum, G., Reflectance Spectroscopy, Springer-Verlag, New York, 1969.

17. Graf, R.T., Koenig, J.L., Ishida, H., Anal. Chem., Vol. 56, p. 773, 1984.

18. Ishida, H., and Koenig, J.L., J. Polym. Sci., Polym. Phys. Ed., Vol. 18, p. 233, 1980.

19. Ishida, H., and Koenig, J.L., J. Polym. Sci., Polym. Phys. Ed., Vol. 18 p. 1931, 1980.

20. Boerio, F.J., Gosselin, C.A., Dillingham, R.G., and Liu, H.W., Analysis of Thin Films on Metal Surfaces, J. Adhesion, Vol. 13, pp. 159-176, 1981.

TECHNICAL REPORT STANDARD TITLE PAGE

1. Report No. 86-6	2. Government Accession No.	3. Recipient's Catalog No.
4. Title and Subtitle Chemical Bonding Technology: Direct Investigation of Interfacial Bonds		5. Report Date January 1986 6. Performing Organization Code
7. Author(s) J. Koenig		8. Performing Organization Report No.
9. Performing Organization Name and Address JET PROPULSION LABORATORY California Institute of Technology 4800 Oak Grove Drive Pasadena, California 91109		10. Work Unit No. 11. Contract or Grant No. NAS7-918 13. Type of Report and Period Covered JPL Publication
12. Sponsoring Agency Name and Address NATIONAL AERONAUTICS AND SPACE ADMINISTRATION Washington, D.C. 20546		14. Sponsoring Agency Code

15. Supplementary Notes Sponsored by the U.S. Department of Energy through Interagency Agreement DE-AI01-85CE89008 with NASA; also identified as DOE/JPL 1012-120 and as JPL Project No. 5101-284 (RTOP or Customer Code 776-52-61).

16. Abstract

This is the third Flat-Plate Solar Array (FSA) Project document reporting on chemical bonding technology for terrestrial photovoltaic (PV) modules. The impetus for this work originated in the late 1970s when PV modules employing siliconne encapsulation materials were undergoing delamination during outdoor exposure. At that time, manufacturers were not employing adhesion promoters and, hence, module interfaces in common with the siliconne materials were only in physical contact and therefore easily prone to separation if, for example, water were to penetrate to the interfaces. Delamination with siliconne materials virtually vanished when adhestion promoters, recommended by siliconne manufacturers, were used. This report describes the activities related to the direct investigation of chemically bonded interfaces.

17. Key Words (Selected by Author(s))	18. Distribution Statement
Organic Chemistry	Unclassified-unlimited

19. Security Classif. (of this report)	20. Security Classif. (of this page)	21. No. of Pages	22. Price
Unclassified	Unclassified	54	